processes

MDPI

*Review*

# A Review on Ionic Liquids in the Design of Carbon-Based Materials for Environmental Contaminant Removal

**Tamara Terzić [1], Tatjana Mitrović [2], Marija Perović [3] and Tamara Lazarević-Pašti [1,*]**

[1] VINČA Institute of Nuclear Sciences - National Institute of the Republic of Serbia, University of Belgrade, Mike Petrovica Alasa 12–14, 11000 Belgrade, Serbia; tamara.tasic@vin.bg.ac.rs
[2] Institute of Physics - National Institute of the Republic of Serbia, Pregrevica 118, 11060 Belgrade, Serbia; tmitrovic@ipb.ac.rs
[3] Jaroslav Černi Water Institute, Jaroslava Černog 80, 11226 Belgrade, Serbia; marija.perovic@jcerni.rs
* Correspondence: tamara@vin.bg.ac.rs

**Abstract**

Contamination of water and soil with a wide range of pollutants, including pesticides, pharmaceuticals, and industrial chemicals, remains a significant environmental challenge. Carbon-based materials are widely recognized for their high adsorption capacity, chemical stability, and the possibility to tailor their surface and structural properties. In recent years, ionic liquids (ILs) have been explored as useful media and functionalization agents in the preparation of such materials. Their unique physicochemical properties can facilitate activation, influence pore structure, and introduce specific functional groups that improve interactions with target contaminants. This review summarizes recent developments in the use of ILs for the synthesis, modification, and regeneration of carbonaceous adsorbents. Particular attention is given to IL-assisted activation techniques, surface functionalization strategies, and reported improvements in adsorption performance. Key challenges, such as the environmental impact and cost of ILs, as well as prospects for developing more sustainable IL-based processes, are also discussed. Taken together, these findings highlight the relevance of IL-enabled carbon materials for practical adsorption processes, including water and wastewater treatment, selective pollutant removal, and regeneration-driven purification systems.

**Keywords:** heteroatom doping; hierarchical porosity; interfacial engineering; sustainable carbon synthesis; adsorptive remediation

## 1. Introduction

The contamination of water and soil with a wide range of pollutants, including pesticides, pharmaceutical residues, industrial solvents, and heavy metals, remains one of the central environmental challenges [1]. Many of these substances are chemically stable, biologically active, and persistent, which makes them resistant to conventional remediation methods. Their continuous presence in natural systems threatens aquatic life [2–7], disrupts food chains [8–10], and poses risks to human health [11–14]. Because of this, there is a growing demand for technologies that can combine efficiency, selectivity, and sustainability in the removal of hazardous compounds.

Carbon-based materials are among the most intensively studied solutions in this context. Their high surface area and chemical stability provide a robust basis for adsorption

Academic Editor: Wen-Tien Tsai

Received: 12 December 2025
Revised: 11 January 2026
Accepted: 18 January 2026
Published: 19 January 2026

processes [15], while their structure can be engineered to interact with specific contaminants [16]. Conventional activated carbon is already widely used in practice [17–22], whereas other distinct forms of carbonaceous materials, including graphene [23,24], carbon nanotubes (CNTs) [25,26], and biochars [27–32], have also demonstrated considerable potential. The challenge that remains is how to tailor these materials to maximize performance while keeping production scalable and environmentally responsible. In recent years, ionic liquids have emerged as valuable allies in this effort. Although originally explored as alternative solvents [33,34], their unusual combination of low volatility, thermal stability, and structural tunability [35] has allowed them to find roles well beyond traditional chemistry. In the field of carbon material design, ionic liquids can act as carbon precursors that undergo direct carbonization into porous solids [36], as surface modifiers that become adsorbed onto carbons and alter their reactivity [37], or as agents that participate in activation processes and influence pore development [38]. Each of these pathways offers opportunities to obtain carbon materials with properties difficult to achieve with more conventional methods.

While several reviews have addressed the general use of ionic liquids in materials science [39–41], comprehensive discussions that specifically examine their role in the preparation of carbon adsorbents remain limited. In particular, the literature often treats carbonization [42], adsorption of ionic liquids on carbon surfaces [43], and ionic-liquid-assisted activation as separate topics, without integrating them into a broader perspective on environmental remediation. This fragmentation makes it difficult to identify the common principles and challenges that connect these approaches. By bringing these aspects together, this review aims to clarify how ionic liquids contribute to the design of carbon-based materials, the advantages they offer over conventional methods, and the main research gaps. The discussion emphasizes how different uses of ionic liquids shape porosity, surface chemistry, and ultimately adsorption efficiency, while at the same time considering the practical issues of environmental safety and cost. By approaching the topic in this way, we aim to offer a more connected understanding of the field and to indicate where further research efforts may be most effectively directed.

## 2. Carbonization of Ionic Liquids

The conversion of ionic liquids into carbon materials relies on the thermal stability and chemical diversity of these salts [44,45]. In contrast to conventional organic precursors such as polymers or biomass, ionic liquids are already composed of cations and anions that contain heteroatoms, aromatic rings, and functional groups [46,47]. When subjected to high temperatures in an inert atmosphere, they undergo a sequence of decomposition, rearrangement, and condensation reactions that ultimately lead to the formation of a carbonaceous structure [44]. The process generally begins with the thermal decomposition of the ionic liquid. At lower carbonization temperatures (300–500 °C), volatile components are released, and the ionic liquid starts to lose its molecular identity. Cations and anions fragment into smaller species, many of which are rich in nitrogen, sulfur, or phosphorus. As the temperature increases, these fragments condense and polymerize, generating an extended network of carbon atoms with heteroatom functionalities embedded in the structure. The preservation of heteroatoms during this stage is one of the defining features of IL-derived carbons, and it differentiates them from carbons obtained from simple hydrocarbon precursors [44,45].

### *2.1. Influence of IL Type on the Structure and Porosity of Carbon Materials*

The nature of the ionic liquid strongly influences the carbonization pathway. The choice of cation and anion determines the type and amount of heteroatoms retained, which in turn affects the thermal decomposition temperature, the extent of aromatization,

and the final carbon yield [46,48]. In many cases, subtle changes in the alkyl side chains or the counterion can result in significant differences in pore structure and surface chemistry [45,48].

Another dimension of this influence is the development of porosity [48]. Some ionic liquids inherently favor the generation of micropores as their bulky cations or anions decompose and leave behind voids [49]. Others require the use of templates such as silica nanoparticles or polymer matrices to produce hierarchical pore systems [50]. In both cases, the liquid nature of ILs ensures homogeneous mixing with additives or templates, which allows better control over the morphology of the resulting carbon.

Among the different classes of ionic liquids, imidazolium-based salts are the most widely studied precursors. Their aromatic heterocyclic cations are relatively stable under pyrolysis, which favors the incorporation of nitrogen into the carbon lattice [51]. As a result, imidazolium-derived carbons typically exhibit nitrogen doping, often associated with improved electronic conductivity and enhanced affinity toward metal ions and polar organic molecules [51,52]. Their textural properties are also favorable for adsorption, with microporosity being particularly pronounced when short-chain imidazolium salts are used [51]. Phosphonium ionic liquids, in contrast, tend to produce carbons enriched with phosphorus functionalities [53]. These groups can act as Lewis acidic sites [53], which alter the surface charge and promote specific interactions with oxyanions and certain industrial pollutants. In some reports, phosphonium-derived carbons have been shown to exhibit a broader and more heterogeneous pore size distribution than their imidazolium analogues. This trend is often linked to differences in the decomposition pathways of the respective cations [37,48].

The choice of an anion is equally important. Sulfonate- and thiol-containing anions have been reported to yield sulfur-doped carbons, which exhibit a strong affinity for soft metal ions such as mercury and lead [54,55]. In addition, sulfur functionalities may enhance hydrophobic interactions with certain organic contaminants, thereby increasing adsorption selectivity [56]. Halide anions, on the other hand, generally do not contribute functional heteroatoms but can influence decomposition temperature and carbon yield [57]. Emerging attention has also been given to choline-based ionic liquids, which are often regarded as more environmentally friendly [58]. Their decomposition produces carbons with both nitrogen- and oxygen-containing surface groups [59], though typically with lower surface area than those obtained from imidazolium salts. Nevertheless, their lower toxicity and cost make them attractive candidates for developing more sustainable IL-derived carbons.

### *2.2. Tailoring Surface Functional Groups During Carbonization*

Beyond the inherent composition of ionic liquids, the conditions under which carbonization is carried out play a decisive role in determining the type and distribution of surface functional groups. Temperature, heating rate, and the surrounding atmosphere all influence whether heteroatoms remain incorporated in stable configurations or are released as volatile species [60,61]. For example, carbonization under nitrogen or ammonia flow can stabilize nitrogen functionalities such as pyridinic and graphitic nitrogen [60,62]. In contrast, carbonization in the presence of carbon dioxide may favor oxygen-rich surface groups [63]. By adjusting these parameters, it becomes possible to deliberately enrich the carbon surface with functionalities that promote specific adsorption mechanisms.

Another approach to tailoring functional groups involves the controlled combination of ionic liquids with additives before carbonization. Mixing ionic liquids with nitrogen- or sulfur-rich precursors can amplify the incorporation of these heteroatoms [64,65], while templating agents or mineral salts may alter the availability of reactive sites on the carbon surface. Post-carbonization treatments, such as mild oxidation or reduction, further

extend the range of possibilities by selectively introducing or stabilizing groups like hydroxyl, carboxyl, or thiol moieties [63,66]. The ability to design surface chemistry in this way is directly linked to adsorption performance. Carbons with basic nitrogen groups tend to interact more strongly with heavy metal ions [67], while oxygen-containing groups favor hydrogen bonding with organic pollutants [68]. Similarly, sulfur functionalities can improve affinity for soft metal ions and hydrophobic organic molecules [69]. Thus, the carbonization of ionic liquids offers not only a route to doped carbon structures but also a means of fine-tuning surface chemistry to match the requirements of different environmental contaminants.

### *2.3. Benefits and Limitations of IL-Derived Carbons*

As mentioned, one of the most important benefits of carbons obtained from ionic liquids is the ability to introduce heteroatoms directly during synthesis [70]. Conventional precursors often yield nearly pure carbon [71] and require post-synthetic doping, while ionic liquids naturally contain nitrogen, sulfur, phosphorus, or oxygen. This results in materials with built-in functionalities that enhance interactions with a wide variety of pollutants. The liquid state of the precursors also allows homogeneous contact with additives and templates, enabling the creation of complex morphologies and hierarchical porosity that are difficult to achieve with solid precursors [44]. Another advantage lies in the tunability of ionic liquids themselves. By choosing different cation–anion combinations, it becomes possible to tailor both the surface chemistry and the pore structure of the resulting carbon. This chemical flexibility is particularly valuable in environmental applications, where selective adsorption is often more important than simply achieving a high surface area. The high chemical and thermal stability of IL-derived carbons [48] further supports their reusability and potential longevity in practical systems.

Despite these strengths, significant limitations remain. The synthesis of ionic liquids is still relatively expensive compared to traditional carbon precursors such as biomass, polymers, or coal derivatives [72]. Many ionic liquids are also not environmentally friendly: their toxicity, persistence, and potential ecological risks raise concerns about large-scale use [73]. In addition, the carbon yield can vary considerably depending on the chosen ionic liquid, and in some cases, it remains too low to be economically viable [48,74]. Questions of scalability also remain unresolved, as most studies are conducted at laboratory scale, and translation to industrial processes requires not only cost reduction but also process simplification.

### *2.4. Adsorption Applications of IL-Derived Carbons*

Although ionic liquids can be carbonized directly, most adsorption applications reported so far rely on poly(ionic liquid) precursors or combinations of ionic liquids with templates and additives. These approaches provide higher yields, better control over porosity, and more accessible surface functionalities [36], which are essential for effective removal of pollutants such as dyes, heavy metals, and pharmaceuticals. By contrast, carbons obtained from the direct carbonization of neat ionic liquids have been investigated primarily for $CO_2$ capture [36,75] and electrochemical energy storage [76], while their use in environmental adsorption remains almost unexplored. This discrepancy highlights a clear research gap: despite the chemical diversity and heteroatom-rich structures of many ionic liquids, their potential as stand-alone precursors for adsorbents targeting pesticides, pharmaceutical residues, or industrial dyes has yet to be systematically assessed. Expanding studies in this direction could reveal whether the simplicity of neat IL carbonization can be translated into practical sorbents for contaminant removal, or whether hybrid and templated strategies will remain indispensable for environmental applications.

## 3. Interactions of Ionic Liquids with Carbon Materials

Adsorption of ILs onto pre-formed carbon materials represents a fundamentally different functionalization strategy from IL-derived carbon synthesis. In this approach, the carbon matrix remains structurally unchanged, while the IL becomes immobilized at its surface. The IL layer can modify surface polarity, enrich the material with heteroatom-containing groups, improve colloidal stability, and introduce new affinity sites relevant for adsorption applications. These interfacial layers are stabilized by a combination of π-π interactions, hydrogen bonding, electrostatic attraction, and dispersion forces, depending on the structures of both the IL and the carbon substrate [77,78]. Because the bulk carbon remains intact, this route provides a versatile and comparatively gentle method to tailor surface chemistry, often resulting in enhanced performance in adsorption, catalysis, composite reinforcement, or interfacial engineering.

### *3.1. Surface Modification Through IL Adsorption*

Surface modification of carbon materials through the adsorption of ILs has been explored across a wide range of carbon architectures, and despite the diversity of systems, several consistent patterns emerge. One example comes from CNT-based materials, where IL adsorption before thermal treatment can substantially alter both mechanical and electronic behavior. Treatment of CNT fibers with the imidazolium IL BMI–I, followed by pyrolysis, produced nitrogen-containing fibers with markedly improved performance: tensile strength increased by more than 100%, the elastic modulus rose severalfold, and the electrical conductivity also improved relative to the pristine fibers [43]. These effects were attributed to the way IL molecules promote interfacial hydrogen bonding between neighboring nanotubes.

Graphene-based materials provide a more detailed view of the molecular origins of these interactions. Computational studies using circumcoronene as a graphene model show that ILs can approach the carbon surface through several structural regions, including the imidazolium ring, alkyl substituents, and even the accompanying anion [79]. Binding is consistently stronger for imidazolium cations than for aliphatic ammonium analogues, underscoring the role of π-π interactions between the aromatic ring and the graphene plane. Additional Density Functional Theory (DFT) and Ab Initio Molecular Dynamics (AIMD) simulations reveal that IL-graphene equilibrium distances typically lie between 3.5 and 4.0 Å, characteristic of strong physisorption, largely driven by dispersion forces [80,81]. The high polarizability of anions such as hexafluorophosphate anion ($PF_6^-$) and bis(trifluoromethylsulfonyl)imide anion ($Tf_2N^-$) further stabilizes these interfacial complexes, and small but measurable charge redistribution between the IL and the carbon surface has been observed [77,78].

Graphene oxide (GO) tends to respond even more strongly to IL modification, mainly because of its abundant oxygen-containing surface groups. IL-modified GO materials show improved dispersion stability and enhanced reusability, and several studies report substantially higher adsorption capacities for organic pollutants compared with unmodified GO [82,83]. The presence of an imidazolium ring or additional amino functionalities in the IL provides complementary interaction sites (hydrogen bonding, electrostatic attraction, and π-π interactions), resulting in stronger binding of dye molecules and other aromatic adsorbates. For many GO-IL hybrids, adsorption behavior follows Langmuir isotherms and pseudo-second-order kinetics, a trend attributed to the formation of a more homogeneous layer of active sites introduced by the IL [84].

Activated carbon (AC) also exhibits clear signatures of IL adsorption. FTIR spectra of IL-functionalized AC commonly reveal new vibrational bands associated with interactions between IL functional groups and the carbon surface (Figure 1) [85]. These

modifications typically correlate with improved adsorption performance, as ILs introduce additional affinity groups not present on the original carbon material.

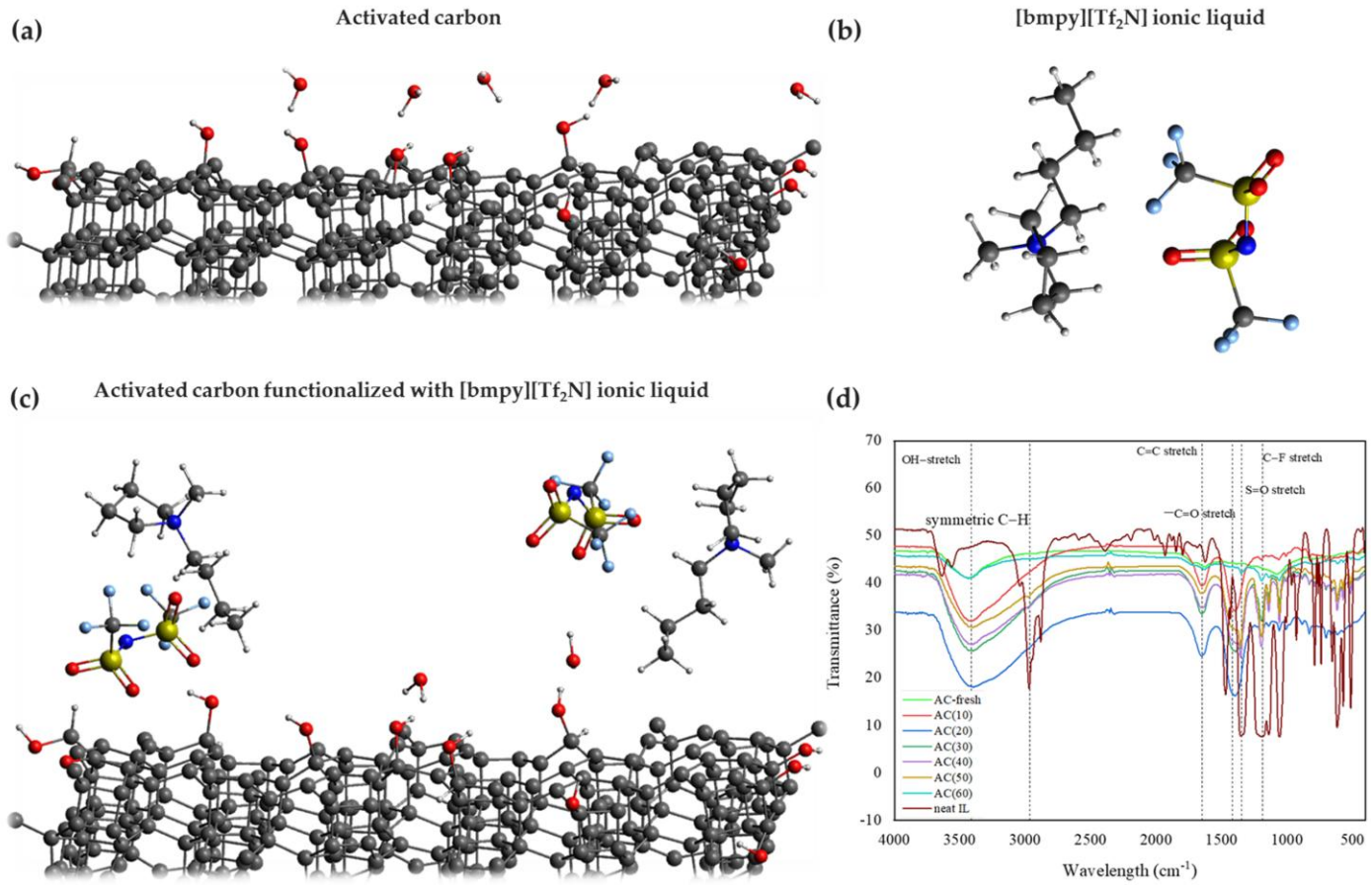


**Figure 1.** Schematic representation of the interaction of activated carbon (**a**) with [bmpy][Tf2N] ionic liquid (**b**) (grey—carbon, red—oxygen, white—hydrogen, blue—nitrogen, yellow—sulfur, light blue—fluorine). Upon the interaction, the activated carbon surface remains intact, while the moisture level is reduced (**c**). This was confirmed by FTIR spectroscopy (**d**), as presented in reference [85]. Dominant groups on the activated carbon surface were hydroxylic ones, whose characteristic peak was reduced in intensity due to water loss upon adsorption of the ionic liquid. Reference [85] is an open access article distributed under the terms and conditions of the Creative Commons Attribution (CC BY) license.

Carbon fibers provide yet another context in which IL adsorption plays a significant interfacial role. When used as sizing agents, imidazolium ILs enhance interfacial shear strength in epoxy composites, and this effect becomes even more pronounced when combined with prior oxidative surface activation of the fibers [86]. π-π stacking between the imidazolium ring and the $sp^2$-hybridized carbon surface appears to be central to this behavior, and comparative studies with hydrophobic and hydrophilic ILs show that differences in ion pairing and surface affinity result in measurable differences in interfacial responses [87]. To place these interactions in a broader materials context, it is instructive to compare imidazolium-carbon π-π stacking with analogous interactions in other porous frameworks. In $sp^2$-rich carbon materials such as graphene or activated carbons, π-π stacking between the imidazolium ring and the delocalized carbon surface is largely governed by dispersion forces and surface polarizability, resulting in non-directional yet extended interfacial contact [88]. In contrast, in porous crystalline systems such as covalent organic frameworks (COFs) or metal–organic frameworks (MOFs), π-π interactions typically occur between discrete aromatic linkers and are constrained by the rigid lattice

geometry, leading to more localized and orientation-dependent binding [89]. Moreover, in MOFs the presence of metal nodes often shifts the dominant interaction mechanism toward coordinative bonding or electrostatic interactions rather than pure π-π stacking [90]. As a consequence, π-π interactions in IL-carbon systems are generally more flexible and surface-adaptive, which is particularly advantageous for adsorption processes involving structurally diverse contaminants.

A common theme in all these systems is that ILs reshape the immediate environment at the carbon surface. Once adsorbed, they form an interfacial layer whose chemical character depends on the IL structure and the type of carbon substrate. This layer can shift the local electronic density, introduce new binding motifs, or strengthen existing interactions. What matters is that these changes occur without disturbing the underlying carbon framework. In practice, this makes IL modification a practical way to fine-tune surface chemistry and adjust the behavior of carbon adsorbents toward particular classes of contaminants.

### *3.2. Interactions Between ILs and Carbon Surfaces*

Interactions between ILs and carbon surfaces arise from a combination of short- and long-range forces, and their balance depends strongly on both the structure of the ionic liquid and the chemical character of the carbon substrate. Aromatic cations, most notably imidazolium species, readily occupy in π-π and cation–π interactions with graphitic domains, a feature consistently observed in experimental systems and supported by extensive computational work [78,79]. These contacts are complemented by dispersion interactions, which often dominate the overall binding energy, especially in systems involving highly polarizable anions such as $PF_6^-$ or $Tf_2N^-$ [80,81]. On oxidized carbon surfaces, hydrogen bonding and electrostatic interactions become equally important due to the abundance of oxygen-containing groups. It enables IL cations to interact with deprotonated carboxylates or to form directional hydrogen bonds with hydroxyl and epoxy functionalities [91,92]. Across different carbon architectures, the interplay of π-π interactions, hydrogen-bonding, and electrostatic forces produces stable interfacial layers that significantly reshape the distribution, polarity, and accessibility of adsorption sites. These interactions are strongly surface-specific. On graphene, IL adsorption is governed mainly by π-π stacking and dispersion forces, with imidazolium cations binding more strongly than aliphatic ammonium counterparts, and with the curvature of the carbon surface modulating binding strength, as shown in comparative studies on graphene sheets and CNTs [43,93]. On GO, the situation is more complex (Figure 2). π-π interactions from the IL cation overlap with hydrogen bonding and electrostatic attraction, often increasing the intersheet spacing and stabilizing the GO layers in aqueous media [82]. Both covalent and noncovalent routes have been used to immobilize IL moieties on GO, including acylation, silanization, and epoxide ring opening [94]. Still, noncovalent assemblies remain particularly attractive because they preserve the $sp^2$ framework and maintain favorable electronic properties. Similar effects are observed on oxidized CNTs, where quaternary ammonium cations interact with surface carboxylates and hydroxyl groups, while both the cation and anion can engage in π-π interactions with the nanotube walls [95]. Sorption studies further show that CNTs with smaller diameters and larger specific surface areas bind ILs more strongly, and that longer alkyl chains enhance Van der Waals contributions, producing a clear correlation between IL structure and binding affinity [92].

In IL-modified chitosan/GO or magnetic biochar composites, Cr(VI) uptake is driven by hydrogen bonding and electrostatic attraction, with reported adsorption capacities exceeding 100–200 mg $g^{-1}$ and rapid kinetics consistent with pseudo-second-order behavior [96,97]. In systems designed for organic pollutants, the IL cation often plays the central role: aromatic rings support π-π interactions with dye molecules or pharmaceuticals,

while hydrogen-bond-donating or accepting groups on the IL introduce additional specificity [98,99]. GO-based IL composites regularly outperform pristine GO, with capacities surpassing 400 mg $g^{-1}$ for certain dyes, and poly(ionic liquid)s (PIL)-functionalized graphene has achieved even higher uptake values, approaching 1900 mg $g^{-1}$ for cationic dyes [100]. IL modification can also shift the preferred adsorption sites on the carbon surface, as shown in theoretical analyses of biochar modified with amino-functional ILs, where the interaction geometry between tetracycline and the IL-modified biochar differed significantly from that observed on the unmodified material, leading to stronger binding and higher removal efficiencies [101].

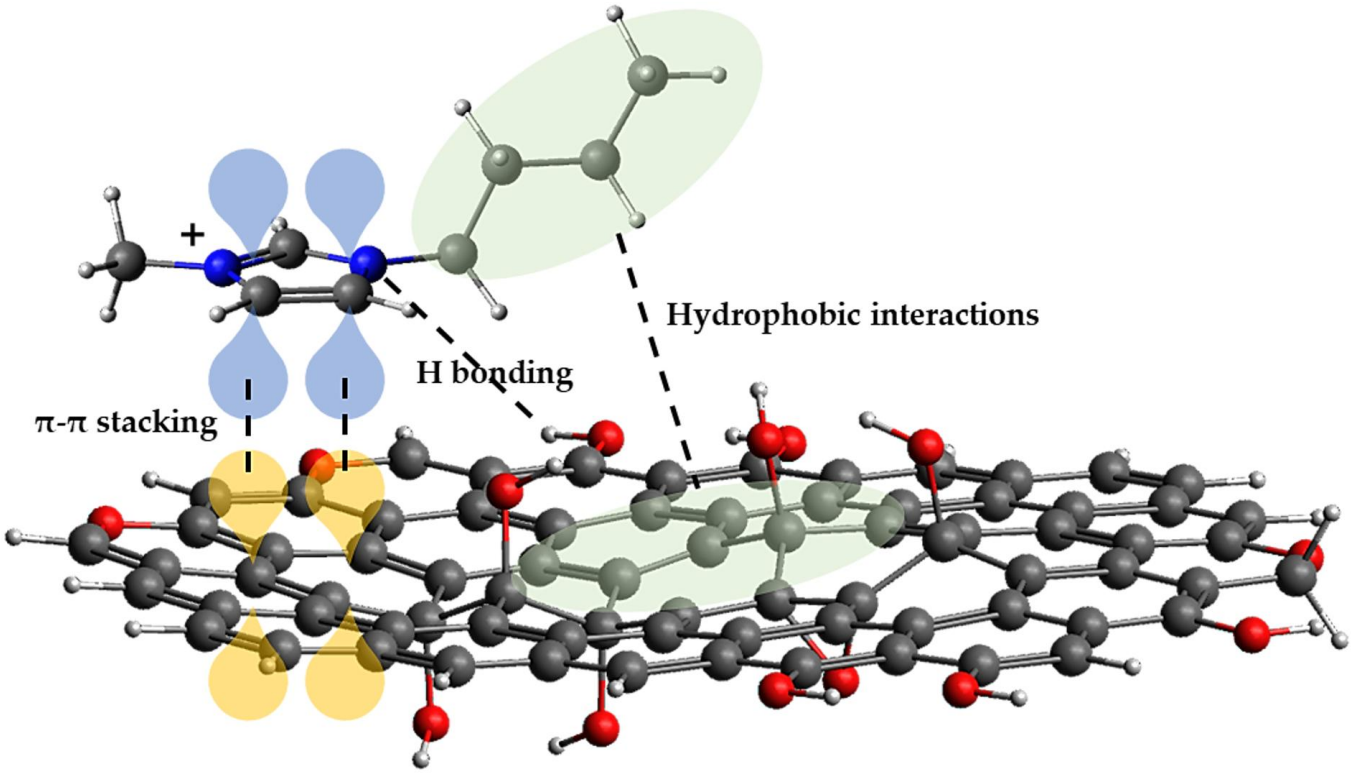


**Figure 2.** Noncovalent functionalization of GO with ILs (grey—carbon, red—oxygen, white—hydrogen, blue—nitrogen).

### *3.3. Effects of IL Functionalization on Selectivity and Adsorption Capacity*

Even when present as thin interfacial layers, ILs can shift the dominant sorption mechanisms from simple π-π stacking or pore filling to ion-pairing, hydrogen bonding, and targeted electrostatic recognition, thereby enabling selectivity that pristine carbon sorbents rarely achieve. Because the structure of an IL can be tuned through independent variation in the cation and anion, the resulting sorbents can be designed to preferentially bind specific classes of contaminants, including pesticides, pharmaceuticals, heavy metals, and per- and polyfluoroalkyl substances (PFAS).

Covalent or noncovalent attachment of ILs onto GO, CNTs, silica-GO hybrids, or AC changes the local electrostatic landscape and introduces new functional moieties. Hydrophilic imidazolium groups, quaternary ammonium cations, sulfonate-containing anions, or long alkyl chains can each favor different interactions. For example, tailored IL coatings on GO@$SiO_2$ adjust the d-spacing and surface polarity, enabling selective extraction of carbamates, triazines, and benzimidazoles from complex matrices [102]. Similarly, covalently grafted ILs onto GO membranes stabilize the interlayer structure via cation–π interactions and enhance size- and charge-based selectivity during filtration [103].

Modifying the surface charge is particularly effective for metal oxyanion adsorption. Aliquat-336 on exfoliated GO forms ion pairs with $HCrO_4^-$ at low pH, and the pH-dependent shift in the material's point of zero charge directly governs chromium uptake [97,104]. Comparable behavior appears in IL-modified biochar, where amino-acid-based ILs strengthen hydrogen bonding with tetracycline and shift the preferred adsorption sites relative to the unmodified material [101]. For anionic contaminants, ILs act as liquid-phase ion exchangers when dispersed on porous carbon surfaces. Studies on IL-impregnated AC show that IL films promote selective replacement of the IL's original anions with PFAS, giving 1.4–2-fold higher uptake than pristine AC even in the presence of dissolved organic matter and divalent cations [105,106]. More hydrophobic or bulky IL anions (e.g., $PF_6^-$, $Tf_2N^-$) similarly enhance affinity for hydrophobic organic pollutants through combined electrostatic and dispersive interactions.

In dyes and pharmaceuticals, aromatic cations capable of π–π interactions and hydrogen-bonding groups in ILs often determine selectivity. Magnetic GO composites modified with ILs display higher adsorption capacities for anionic dyes due to strengthened electrostatic attraction [107], while PIL-functionalized graphene reaches capacities near 1900 mg $g^{-1}$ for methylene blue owing to synergistic π-π interactions and hydrogen bond interactions [100]. IL-$SiO_2$-GO composites also achieve high Pb(II) and As(III) removal, reflecting the presence of multiple coordination sites introduced by the IL-assisted synthesis route [108].

Under optimized conditions, IL-modified ACs can retain or even improve $CO_2$ adsorption at elevated temperatures, where reduced surface tension allows ILs to distribute more uniformly and maintain access to inner pores [109]. Similar trends are observed in magnetic GO composites, where IL layers introduce new sorption sites without fully obstructing the carbon framework, enabling high capacities for arsenic, heavy metals, and dyes, along with excellent reusability [110,111].

It should be noted that the role of pH in IL-modified carbon systems is highly system-specific and governed by a coupled response of the ionic liquid functionality, carbon surface chemistry, and contaminant speciation. In many reported systems, pH primarily modulates electrostatic interactions and ion-exchange equilibria rather than the intrinsic adsorption capacity introduced by IL functionalization. As a result, pH effects are typically discussed within individual case studies rather than generalized across IL-carbon systems.

## 4. Activation of Carbon Materials Using Ionic Liquids

The role of ILs in carbon synthesis extends far beyond simple surface modification (Figure 3). They can participate directly in the activation and structural development of carbon materials during carbonization due to their negligible vapor pressure, structural tunability, and high thermal stability. In this context, ILs function simultaneously as carbon precursors, heteroatom dopants, reaction media, and pore-forming agents, enabling routes to porous carbons that differ fundamentally from conventional activation methods [112]. Their fluid nature ensures homogeneous mixing, while their decomposition facilitates in situ generation of meso- and macropores, often assisted by eutectic salt systems [113] or by IL-template co-assembly routes [114]. As a result, IL-assisted activation can tune pore size distribution, increase specific surface area, and introduce well-dispersed N, S, P, B, and O functionalities directly into the carbon framework. This ability to simultaneously control porosity and heteroatom chemistry gives IL-based activation a unique position among carbon-processing strategies. In many systems, the IL determines whether the resulting carbon is predominantly microporous or hierarchically porous [70], while also influencing conductivity, graphitization, and dopant retention, properties essential for adsorption, catalysis, and electrochemical storage.

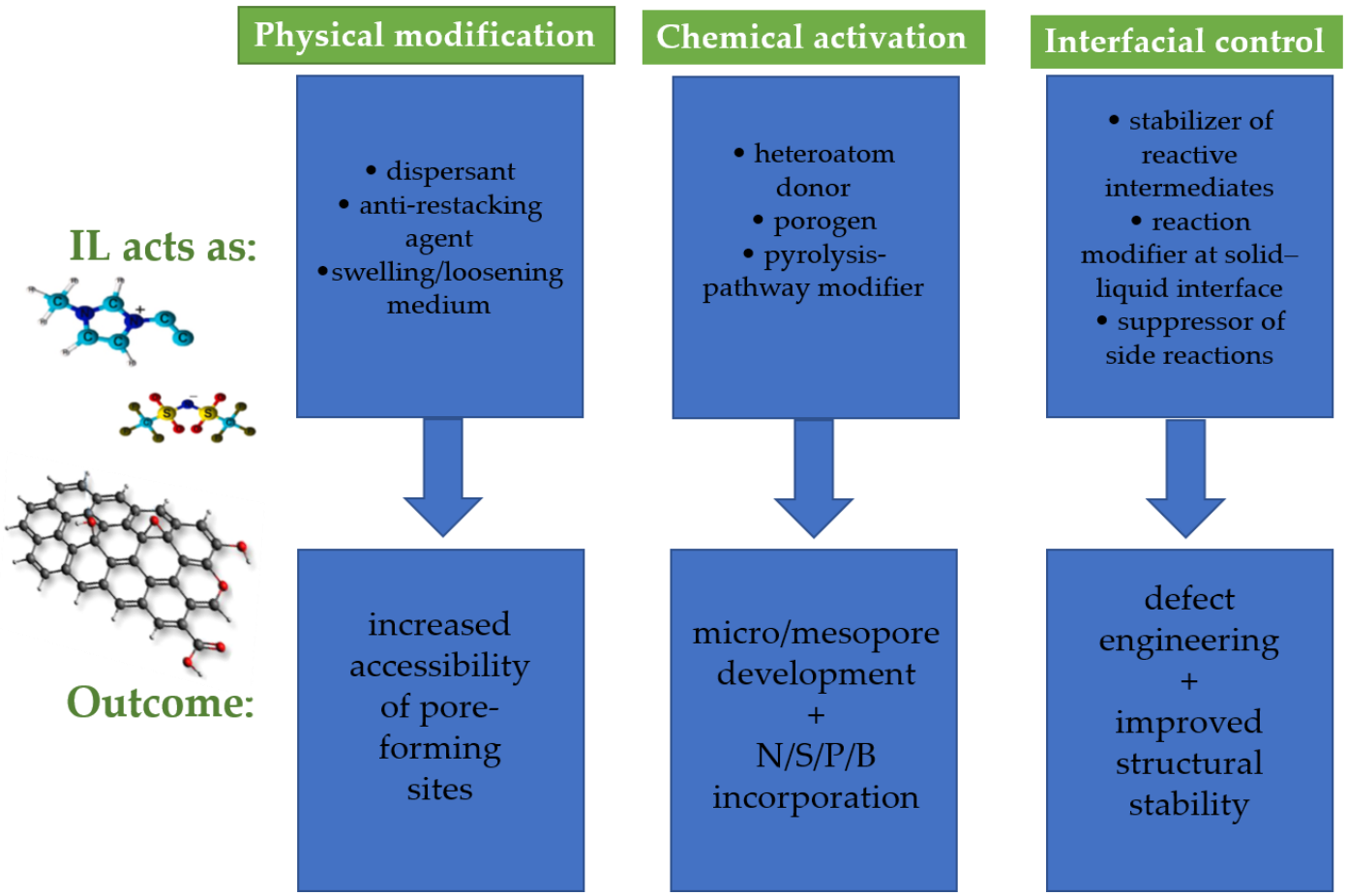


**Figure 3.** Schematic representation of IL-assisted physical, chemical, and interfacial modification pathways.

*4.1. IL-Assisted Activation Methods*

ILs can promote exfoliation, dispersion, or structural loosening of layered carbon precursors, thereby facilitating the development of accessible porosity. For materials such as graphene and CNTs, which are typically prone to π-π stacking, ILs suppress aggregation by shielding graphitic domains and stabilizing the exfoliated state [115]. This behavior supports their use in preparing cellulose/graphene or cellulose/CNT composites, where the IL serves as both a solvent and a dispersant, enabling the formation of highly integrated hybrid networks. ILs can also function as porogens, where their decomposition or ion-mediated reactions guide the formation of micro- and mesoporous architectures. Several ILs accelerate pore formation by disrupting the carbon matrix or participating in reactions that generate gaseous species, thereby creating micro- and mesopores. In some cases, the IL anion itself acts as a porogen [116]. Related approaches use ILs in combination with halide or pseudohalide salts to activate GO at mild temperatures, enabling heteroatom functionalization such as fluorination [117].

Beyond physical effects, ILs participate in chemical activation by serving as heteroatom sources and by modifying the decomposition and carbonization pathways of various precursors. A widely used strategy involves adding ILs to biomass, polymers, graphene, or GO to introduce nitrogen, sulfur, phosphorus, or boron during thermal treatment. Even small IL loadings can significantly alter the resulting carbon's surface chemistry, enabling materials with improved conductivity, redox activity, or adsorption performance [42]. Electrochemical routes further expand this concept. rGO/IL composites synthesized in situ can enhance charge storage or catalytic behavior due to the combined effects of heteroatom incorporation and stabilized graphitic domains [118].

At solid–liquid interfaces, ILs influence activation by stabilizing intermediates, suppressing undesired reactions, and altering surface chemistry during electrochemical or thermal treatments. Under electrochemical or thermal conditions, ILs can participate in interfacial reactions that modify both the precursor and the IL itself, generating new functionalities or stabilizing intermediates. Studies of graphene/tetracyanoborate IL interfaces show that ILs can alter decomposition pathways, suppress undesirable reactions, and improve safety margins in energy-storage applications [119]. These interfacial processes are increasingly recognized as contributors to controlled activation, graphitic defect engineering, and enhanced structural stability.

### *4.2. Control of Pore Structure and Specific Surface Area*

ILs allow fine control over the pore architecture of carbon materials by regulating nanosheet spacing, suppressing graphitic restacking, and directing the development of micro-, meso-, and macropores during carbonization or impregnation. In graphene-based systems, cation–π and π-π interactions between ILs and graphitic domains prevent the collapse of lamellar structures, enabling the formation of exfoliated frameworks that would otherwise aggregate in the absence of ILs. This principle is exemplified in IL-derived bulky gels, where the IL stabilizes dispersed graphene layers and, upon carbonization, yields hierarchically porous carbons with simultaneously accessible micro- and mesopore networks. The IL in that way acts as an in situ pore regulator, determining interlayer distance and guiding the emergence of porosity compatible with ion transport [120]. When ILs are introduced post-synthesis, as in the case of ACs, their influence on porosity is concentration-dependent. At low loadings, ILs smooth and homogenize the carbon surface while only moderately reducing the BET surface area. However, higher IL contents progressively infiltrate micropores, decreasing pore volume and specific surface area due to pore blockage. Verma et al. [121] reported that imidazolium ILs impregnated into granular AC fill the smallest pores first, transforming a highly microporous structure into a material dominated by larger, less accessible voids, with a pronounced decline in total porosity at ≥10 wt% IL. Such trends reflect the strong affinity of ILs for microporous domains and their ability to redistribute pore populations through selective occupation. Importantly, even when porosity decreases, ILs can enhance the functional accessibility of the remaining surface. Costa et al. [93] demonstrated that rGO-modified glassy carbon electrodes in contact with an imidazolium IL exhibit substantially higher effective surface area and improved charge transport, confirming that IL–carbon interfaces can improve usable porosity and electrochemical accessibility regardless of geometric surface area.

Beyond simple pore blocking or stabilization, ILs can also direct the formation of tunable porous structures by promoting gel-like assemblies and suppressing nanosheet aggregation in GO and graphene systems. The formation of IL-graphene networks yields carbon materials with increased accessible surface area, improved electrolyte wetting, and porosity tailored to the dimensions of ionic species. These effects demonstrate that ILs act as structure-directing agents capable of expanding, stabilizing, or selectively filling pore domains, providing a level of control over surface area and pore distribution that is difficult to achieve through conventional activation routes [120].

### *4.3. Comparison with Conventional Activation Techniques*

Conventional activation methods, whether physical routes using $CO_2$ or steam, or chemical routes employing agents such as KOH, $ZnCl_2$, and $H_3PO_4$, have long served as the standard for generating porous carbons with high surface areas. Chemical activation is typically preferred due to lower temperature requirements, rapid pore development, and high carbon yields, particularly when alkaline or acidic salts promote dehydration, charring, and matrix expansion during pyrolysis [122,123]. KOH activation, for example,

reliably produces highly microporous carbons with excellent BET surface areas, while $H_3PO_4$ and $ZnCl_2$ favor the development of mesoporosity through dehydration-driven crosslinking and aromatization reactions [123,124]. However, these classical methods have critical drawbacks, including corrosive reagents, high waste-generation during post-washing, limited control over heteroatom incorporation, and environmental or toxicity concerns, most notably for KOH and $ZnCl_2$, which require extensive neutralization and may release hazardous residues into aqueous effluents [122,125].

In contrast, ionic liquids introduce fundamentally different activation pathways. Rather than relying solely on inorganic dehydrating agents, ILs can act simultaneously as dispersants, porogens, heteroatom sources, and structure-directing media, as already mentioned. Their negligible vapor pressures and strong noncovalent interactions with carbon precursors enable controlled exfoliation and stabilization of lamellar structures, mitigating the collapse of graphene- or GO-based frameworks during carbonization, an effect not achievable with standard chemical activators [115]. IL-mediated bulky gels, for instance, preserve unstacked 2D architectures and guide pore formation through ion-mediated templating, producing micro/mesoporous systems with large accessible surface areas and hierarchical connectivity [120]. Moreover, ILs offer molecular-level tunability: by swapping cations, anions, or functional groups, one can selectively introduce N, S, P, or B heteroatoms into the carbon skeleton during pyrolysis, a capability only indirectly achievable with classical activators [42]. This heteroatom doping is central to enhancing conductivity, wettability, and redox activity, properties crucial for adsorption, catalysis, and energy storage applications. Another practical advantage is that IL-assisted activation often occurs at milder conditions and with fewer corrosive byproducts. KOH activation leaves caustic residues that must be neutralized and generates environmentally challenging effluents, while IL-based processes typically avoid large volumes of hazardous waste, and in some instances require no aggressive washing at all. In systems where ILs are combined with conventional activators, the IL can stabilize nanosheet frameworks and promote uniform activation, yielding carbons with better-controlled pore size distributions and higher accessibility for bulky adsorbates or ionic liquid electrolytes [120]. While $ZnCl_2$ activation is known to generate high surface areas, it requires extensive post-leaching to remove ZnO or unreacted salt, and even then, residual zinc species often remain embedded in the carbon structure [125]. IL-based routes avoid many of these issues because the carbon precursor, activator, and dopant can be built into a single molecular framework.

### *4.4. Sustainability and Potential for Industrial Application*

The long-term stability and reusability of IL-modified carbons are central to assessing their sustainability and suitability for industrial deployment. Across a wide range of systems, IL-assisted adsorbents demonstrate robust performance over sequential adsorption–desorption cycles, indicating that the functional interphases formed by ILs are chemically resilient. Magnetic graphene composites modified with ILs, for instance, maintained high removal efficiencies for pharmaceuticals over four cycles, with ibuprofen uptake decreasing only moderately from 98% to 84% and penicillin G from 95% to 86%, suggesting that most IL-carbon interactions withstand chemical regeneration and mechanical handling [126]. IL-derived Mn/N co-doped biochars show similar durability. The incorporation of 1-methyl-3-methylimidazolium tetrachloromanganate ($[Emim]_2[MnCl_4]$) simultaneously enhances porosity and introduces stable heteroatom-binding environments, enabling efficient reuse without structural deterioration [127]. From a sustainability perspective, these findings are encouraging, as they indicate reduced material consumption, lower waste generation, and greater process reliability. IL-mediated fabrication of graphene–cellulose composites further underscores this potential. Composites prepared in ILs maintain structural integrity and functionality under demanding conditions,

including extreme pH and repeated loading, which is essential for continuous-flow water treatment or membrane-based separations [115,128]. Likewise, IL-modified chitosan fibers used for selective Au(I) recovery remain mechanically and chemically intact across multiple cycles, implying that IL-based functional groups are not rapidly depleted or hydrolysed, which is a key requirement for sustainable operation [129].

Despite these advantages, the broader industrial adoption of IL-based activation strategies will depend on selecting ILs that are economically accessible, thermally stable, and environmentally friendly. Protic ILs, amino acid-based ILs, and nitrate-, acetate-, or phosphate-based systems offer favorable profiles due to lower synthesis costs, reduced toxicity, and straightforward recycling compared with fluorinated ILs or those containing bulky hydrophobic anions. When paired with biomass precursors or low-temperature activation routes, these ILs could form the basis of scalable, energy-efficient, and low-waste production pathways for advanced carbon adsorbents.

## 5. Examples of Adsorption Applications

A wide range of IL-functionalized carbon-based adsorbents has been reported, including chitosan- and biochar-based materials, GO and rGO composites, CNT- and AC-supported ILs, as well as IL-modified silica–carbon hybrids. These systems have been applied to the removal of toxic metal ions (e.g., Cr(VI)/Cr(III), Pb(II), Cd(II), Hg(II), As species, rare earth ions, per- and PFAS, anionic and cationic dyes, pharmaceuticals and antibiotics, $CO_2$, and even noble metal cyanide complexes. In most cases, IL functionalization improves adsorption capacity, selectivity toward targeted species, and often reusability of the sorbent compared with the corresponding unmodified carbon material.

From a contaminant-removal perspective, IL-carbon interfacial interactions translate directly into distinct adsorption mechanisms (Figure 4). Electrostatic attraction dominates the uptake of oppositely charged species, such as Cr(VI) oxyanions, PFAS, and anionic dyes, particularly under acidic conditions, when IL-modified surfaces remain positively charged. π-π interactions between aromatic IL cations and graphitic domains enhance the affinity of these cations toward planar organic pollutants, including pharmaceuticals, pesticides, and dyes. Hydrogen bonding contributes to the adsorption of polar molecules such as antibiotics and phenolic compounds, while hydrophobic interactions become increasingly important for nonpolar organics as alkyl chain length increases. In some systems, ion exchange between IL counterions and target contaminants provides an additional removal pathway. Importantly, these mechanisms often operate cooperatively rather than independently, explaining the frequently observed enhancement in both adsorption capacity and selectivity relative to pristine carbon materials. Representative examples are summarized in Table 1, illustrating the diversity of IL precursors, activation routes, and adsorption mechanisms.

The examples summarized in Table 1 reveal consistent trends across different carbon classes and activation strategies. Ionic-liquid-assisted activation and functionalization generally lead to higher specific surface areas, broader pore-size distributions, and enhanced accessibility of active sites compared to pristine carbons. In most cases, these structural modifications translate into improved adsorption capacities, faster kinetics, or enhanced selectivity toward target contaminants. Notably, IL-derived heteroatom doping (particularly N, S, and P) frequently correlates with stronger pollutant–surface interactions and improved regeneration performance. While the magnitude of improvement depends on the IL structure, precursor type, and activation route, the table collectively demonstrates that IL-assisted approaches provide systematic performance gains rather than isolated case-specific effects.

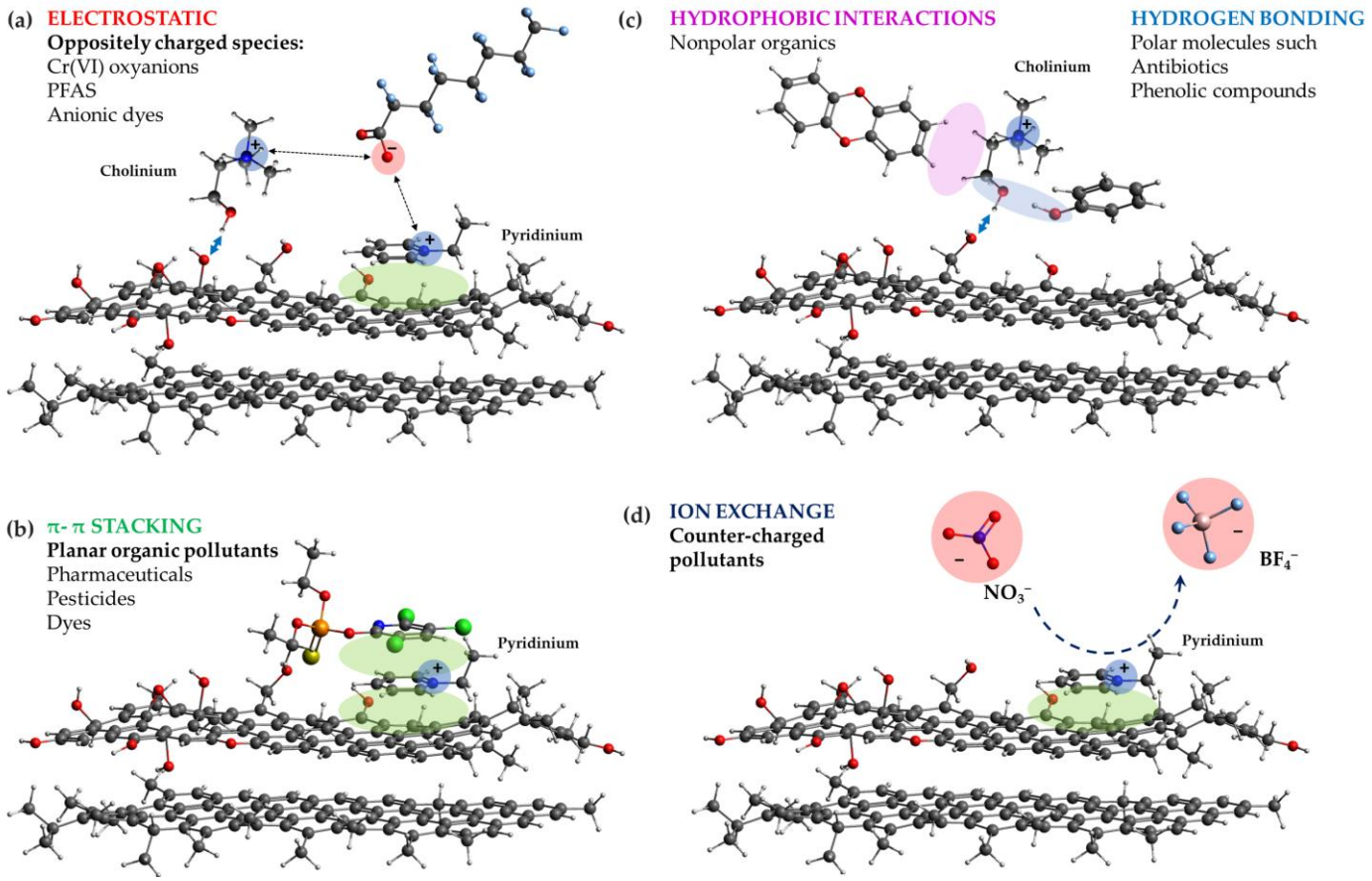


**Figure 4.** Schematic representation of the interaction of IL-modified carbons with different contaminants via: (**a**) electrostatic interactions, (**b**) π-π stacking, (**c**) hydrogen bonding and hydrophobic interactions, and (**d**) ion exchange (grey—carbon, red—oxygen, white—hydrogen, blue—nitrogen, yellow—sulfur, light blue—fluorine, orange — phospohrus). The model surface of carbon is modified with cholinium ion (bonded to the surface via hydrogen bond, marked as a double-sided blue arrow) or pyridinium ion (bonded to the surface via π-π stacking, marked as a green ellipse).

**Table 1.** Representative examples of IL-functionalized carbon materials for environmental contaminant removal.

| Carbon Support | IL Type/Functionalization | Target Contaminant(s) | Adsorption Performance (If Reported) | Dominant Interactions/Advantages | Reference |
|---|---|---|---|---|---|
| MWCNT | Vinyl-pyridinium PIL grafting | Cr(VI) | Up to ~37% removal (12 h) | Electrostatic and π-interactions | [130] |
| Activated carbon | Confined amine-based ILs | $CO_2$ | Improved uptake at elevated T | Chemical affinity + reduced pore blocking | [109] |
| GO laminate | Imidazolium IL (mimG-GO) | Anionic dyes (DR80, RB5, MO) | >99% for DR80, RB5, MO | Cation–π interactions improving membrane stability; controlled interlayer spacing, electrostatic and steric exclusion | [103] |
| Biochar (corn stover biochar, CSB) | Imidazolium IL grafted via trimethoxysilylpropyl linker | $Cd^{2+}$ | $q_e \approx 48.1$ mg $g^{-1}$ (vs. 44.0 mg $g^{-1}$ for raw CSB) | Shifted adsorption sites, stronger H-bonding | [131] |
| Graphene | PIL grafting (poly(1-vinylimidazole) | MB | Up to 1910 mg $g^{-1}$ | Strong π–π interactions, fast kinetics | [100] |
| GO | PIL covalent bonding (P[MATMA][$BF_4$]) | $CO_2$ | 21.54 $cm^3$ $g^{-1}$ at 0 °C and 900 mmHg (vs. 3.07 $cm^3$ $g^{-1}$ for GO) | Increased surface area, abundant $BF_4^-$ sites enabling Lewis acid–base $CO_2$ interactions, enhanced porosity, and affinity | [132] |
| GO | PIL microemulsion composite | MO | $q_{max}$ up to 128 mg $g^{-1}$ | Hydrogen bonding, hydrophobic $PF_6^-$ interactions, improved GO dispersion, and increased adsorption sites | [133] |
| Activated carbon (from mixed recyclable waste) | Phosphonium IL | Hg(II) | $q_{max}$ = 105 mg $g^{-1}$ (vs. ~44 mg $g^{-1}$ for unmodified AC at optimal pH) | Strong coordination/chelation via phosphorus sites in IL + enhanced surface functionality | [134] |
| Activated carbon | Hydrophobic IL grafting | PFAS | Up to ~2.26-times higher removal efficiency (six PFAS in DWTP influent) vs. pristine AC | Anion-exchange (IL sites) + hydrophobic interactions → selective PFAS uptake from real water | [106] |
| Activated carbon | Imidazolium IL impregnation ([$C_2$MIM][$NTf_2$], [$C_6$MIM][$NTf_2$]) | PFAS | 1.4–1.96× higher removal vs. pristine AC in real surface water, lower efficiency in DI water | Anion exchange + IL thin-film partitioning | [105] |
| CNT (MWCNT) | PIL grafting via mussel-inspired PDA + RAFT polymerization ([C16VIm][Br]) | CR | $q_{max}$ = 254.6 mg $g^{-1}$, $q_e \approx$ 176 mg $g^{-1}$ at 56 min; markedly higher vs. pristine CNT (100.9 mg $g^{-1}$) | Electrostatic attraction + π–π stacking (imidazolium ring—CR aromatic system), enhanced dispersibility, dense IL-derived active sites | [135] |
| GO–cellulose composite (CGC) | IL processing in [Bmim]Cl | Ce(III) | $q_{max} \approx$ 109 mg $g^{-1}$ | Ion-exchange mechanism (confirmed by XPS) | [136] |
| GO | Aliquat-336 impregnation (quaternary ammonium IL) | Cr(VI) | $q_{max}$ = 285.71 mg $g^{-1}$, 99.8% removal in 45 min | Ion-pairing, pH-dependent selectivity | [97] |
| MWCNT | IL functionalization (tetra-n-heptylammonium bromide) | Cr(VI)/Cr(III) | $q_{max}$ = 85.83 mg $g^{-1}$, ~99.5% removal at 0.15–0.20 g dose, equilibrium in 40 min | Cation–π, anion–π, electrostatic | [95] |

| | | | | | |
|---|---|---|---|---|---|
| Reduced GO | IL modification | Cr(VI) | $q_{max} \approx 232.55$ mg $g^{-1}$ | Electrostatic and chemical interactions, enhanced adsorption over GO/rGO due to IL functionalization | [137] |
| GO sponge | Imidazolium IL | Cr(VI) | $q_{max} = 208.3$ mg $g^{-1}$ at 23 °C, 99.3% removal of 10 ppm Cr(VI) | Electrostatic attraction + π-electron-assisted reduction of Cr(VI) → Cr(III), hierarchical porous sponge prevents GO restacking and increases accessibility of IL sites | [138] |
| GO | Dicationic IL | Cr(VI) | $q_{max} = 263.8$ -281.5 mg $g^{-1}$ (298–308 K), experimental $q_e \approx 260.9$ mg $g^{-1}$ at pH 3 | Electrostatic attraction between anionic Cr(VI) species and protonated imidazolium $N^+$, combined with partial reduction of Cr(VI) → Cr(III) | [139] |
| GO | Amine-functionalized IL grafting | Phthalates (PAEs) | Adsorption capacities ranged ~266–484 μg $g^{-1}$ (for different PAEs | π–π interactions, hydrophobic interactions with IL alkyl chains, enhanced GO interlayer spacing and increased surface area → improved uptake of hydrophobic phthalates | [91] |
| GO | Imidazolium IL grafting | DR80 | $q_{max} = 500$ mg $g^{-1}$, equilibrium in ~10 min, 99.2% removal retained after 4 cycles | Strong electrostatic, H-bonding, and π–π interactions, IL prevents GO restacking, ultrafast adsorption rate (588 mg $g^{-1}$ $min^{-1}$) | [82] |
| GO | IL 1-hexyl 3-decahexyl imidazolium | Pharmaceuticals (sulfamethoxazole SMZ, carbamazepine CBZ, ketoprofen KET) | Higher adsorption than pristine GO ($q \approx 27.25$ mg $g^{-1}$ for SMZ on GO–IL vs. lower on GO) | Hydrogen bonding + van der Waals + electrostatic/π–π (IL–drug interactions) + improved dispersion of GO in water | [83] |
| GQDs | IL-capped | Cr(VI) | $q_{max} = 934.6$ mg $g^{-1}$ (pH 7) | Electrostatic attraction between protonated IL groups and anionic Cr(VI) species + surface complexation/ion-exchange, IL capping prevents GQD aggregation and increases accessible active sites | [140] |
| $MoS_2$-RGO | Imidazolium IL coating | MB | $q_{max} = 143.9$ mg $g^{-1}$, high removal; reusable ~78% after 5 cycles | Electrostatic attraction + π–π interactions, IL improves dispersion, magnetic separation | [141] |
| GO | PIL functionalization | CR | $q_{max} = 191.9$ mg $g^{-1}$, near-saturation within 5 min | Electrostatic attraction between cationic PIL and anionic CR, π–π stacking; H-bonding; enhanced uptake vs. pristine GO | [142] |
| Spherical activated carbon (SAC) | Polymerized IL (poly(1-vinyl-3-butylimidazolium hexafluorophosphate) | Ibuprofen | ≈2-fold higher adsorption capacity vs. pristine SAC | Improved hydrophobic and electrostatic interactions from the PIL layer | [143] |
| MWCNT | IL-based polyether (poly(1-glycidyl-3-methylimidazolium chloride), PGMIC) | Anionic azo dyes (Orange II, Sunset Yellow FCF, Amaranth) | $q_{max} = 67.57$ mg $g^{-1}$ (Orange II), 85.47 mg $g^{-1}$ (Sunset Yellow), 47.39 mg $g^{-1}$ (Amaranth) at 25 °C, rapid adsorption | Electrostatic attraction + charge neutralization, IL polymer improves CNT dispersion | [144] |

| | | | | | |
|---|---|---|---|---|---|
| GO–$SiO_2$ composite | IL-assisted synthesis | Pb(II), As(III) | $q_{max}$ = 527 mg $g^{-1}$ for Pb(II), $q_{max}$ = 30 mg $g^{-1}$ for As(III), >99% removal within 60 min, stable over 4 cycles | Synergistic porosity + IL-assisted dispersion of GO, electrostatic attraction, ligand exchange, surface complexation | [108] |
| Nanoporous carbon | Task-specific ionic liquid precursors (EBI-T, EBI-B, BBI-T, HBI-T, NBI-T, XBI-T) | $CO_2$ | $CO_2$ uptake = 2.01–3.59 mmol $g^{-1}$ at 0 °C, 1.23–2.49 mmol $g^{-1}$ at 25 °C, surface area 588–1277 $m^2$ $g^{-1}$ (depending on IL precursor) | High N-doping from IL precursors enhances $CO_2$ affinity, IL structure determines microporosity/mesoporosity and adsorption strength, TSILs act as both carbon and heteroatom source | [145] |
| GO-magnetic composite (MGO) | Bifunctional ionic liquid + chitosan grafting (IL/Chit@MGO) | Tetracycline | High loading capacity for aptamer ($5.80 \times 10^{-7}$ mol $g^{-1}$), rapid binding (20 min) | Electrostatic attraction (positive IL/Chit@MGO—negative aptamer), π–π stacking, H-bonding, IL provides selective interaction sites, magnetic separation | [146] |
| GO (electrochemically N/B/F-codoped RGO) | Imidazolium IL precursor ([EMIM][$BF_4$] | Tetracycline | 93% removal (5 mg $L^{-1}$) in 60 min, TOC removal 40% | Nonradical AOP pathways; high electron-transfer efficiency | [147] |

P[MATMA][$BF_4$]—poly[2-(methacryloyloxy)-ethyl] trimethylammonium tetrafluoroborate. DR80—direct 80. RB5—reactive black 5. MO—methyl orange. MB—methylene blue. [$C_2$MIM][$NTf_2$]—1-ethyl-3-methylimidazolium bis(trifluoromethylsulfonyl)imide. [$C_6$MIM][$NTf_2$]—1-hexyl-3-methylimidazolium bis(trifluoromethylsulfonyl)imide. PFAS—per- and poly-fluoroalkyl substances, nonyl-bis-imidazolium cation with the $[Tf_2N]^-$ anion is labelled NBI-T, ethyl-bis-imidazolium cation with the $[BETI]^-$ anion is labelled EBI-B, ethyl-bis-imidazolium cation with the $[Tf_2N]^-$ anion is labelled EBI-T, hexyl-bis-imidazolium cation with the $[Tf_2N]^-$ anion is labelled XBI-T, butyl-bis-imidazolium cation with the $[Tf_2N]^-$ anion is labelled BBI-T, xylyl-bis-imidazolium cation with the $[Tf_2N]^-$ anion is labelled XBI-T.

## 6. Challenges and Future Perspectives

Despite their unique advantages, IL-assisted strategies face non-negligible environmental and economic barriers. It is important to emphasize that the advantages and limitations of IL-assisted strategies are inherently structure-dependent. Imidazolium-based ILs are most frequently employed due to their strong aromatic cations and favorable interactions with graphitic domains, yet they are often associated with higher synthesis cost and, in the presence of fluorinated anions, increased environmental persistence. In contrast, ammonium- and phosphonium-based ILs offer enhanced thermal stability and hydrophobic character, which can be beneficial for gas capture and anion exchange, but their steric bulk may hinder access to microporous carbon domains.

Many widely used ILs, particularly fluorinated imidazolium or phosphonium salts, remain costly to produce, energetically demanding to purify, and poorly biodegradable, raising concerns about large-scale deployment. Thermal processing imposes additional challenges because some ILs decompose extensively at carbonization temperatures or form persistent byproducts, while others require co-activators to achieve meaningful porosity [148]. Moreover, industrial processes would need robust solvent-recovery systems to prevent IL loss and mitigate environmental risk. These constraints do not weaken their scientific value but highlight that IL-assisted activation is most justified when the performance gains, like precise pore tuning, controlled heteroatom incorporation, or nanoscale stabilization, offer clear advantages over conventional activators.

A major direction for future progress lies in designing ILs that reconcile high performance with low environmental impact. Biodegradable cholinium-based ILs, amino acid-derived protic ILs, and ILs synthesized from renewable organic acids already demonstrate reduced toxicity, lower cost, and improved compatibility with biomass precursors. Their structural diversity enables selective heteroatom doping without relying on halogenated anions, while their improved recyclability enhances process sustainability. Further advances are expected from ILs with tunable volatility, dynamic covalent motifs, or self-porogen functionalities that activate carbon precursors without auxiliary reagents. Developing ILs that degrade into benign fragments after processing would substantially strengthen their case for industrial adoption.

It should also be recognized that ionic liquids are not inherently benign, and their toxicity is strongly structure-dependent. Both experimental and theoretical studies indicate that the nature of the cation, alkyl chain length, and anion identity play critical roles in determining ecotoxicity and biodegradability. In particular, longer alkyl chains and fluorinated anions are often associated with increased biological persistence and toxicity, whereas protic, choline-based, and amino-acid-derived ionic liquids exhibit more favorable environmental profiles [149]. These considerations underscore the importance of rational IL design, immobilization strategies, and recycling protocols when assessing the sustainability of IL-assisted carbon materials.

A recent study on IL-based regeneration of activated carbon further illustrates both the promise and the remaining challenges of these systems. While high regeneration efficiencies and multi-cycle stability were achieved, full IL recovery required an additional ABS-mediated separation step, underscoring that large-scale applications will depend on efficient IL recycling strategies and careful management of secondary waste streams [150].

To transition IL-assisted activation from laboratory-scale demonstrations to industrial practice, several challenges must be addressed. First, systematic structure–property relationships are needed to predict how IL composition governs carbon yield, dopant retention, pore hierarchy, and mechanical stability. Second, hybrid activation schemes, combining IL templating with mild chemical or physical activation, offer a promising route to reducing IL consumption while retaining structural precision. Third, scalable recycling protocols must be developed to recover ILs after activation or washing, minimizing waste

and reducing operational costs. Finally, pilot-scale studies are required to evaluate reactor design, heat management, IL stability under continuous operation, and compatibility with biomass feedstocks. With these advances, ILs could evolve from niche precursors to robust tools for producing next-generation carbons tailored for adsorption, catalysis, energy storage, and environmental remediation.

## 7. Conclusions

ILs have emerged as exceptionally versatile tools in the design of advanced carbon materials. Whether used as carbon precursors, structural modifiers, porogens, heteroatom donors, or activating media, ILs provide an unprecedented degree of molecular-level control over carbon architecture. They enable precise tuning of pore size distribution, surface chemistry, and electronic properties that conventional activation methods cannot easily achieve. Their ability to stabilize lamellar precursors, guide hierarchical porosity, and deliver high levels of N, S, P, or B doping places them at the lead of next-generation carbon engineering. Yet, their widespread application will depend on overcoming key practical barriers, including cost, recyclability, and environmental compatibility. Emerging families of biodegradable, bio-derived, and task-specific ILs offer a path forward, making IL-assisted activation increasingly feasible and sustainable. Continued development of greener IL chemistries, combined with mechanistic understanding and scalable process engineering, will determine how rapidly these systems progress beyond laboratory synthesis.

**Author Contributions:** Conceptualization, T.L.-P.; methodology, T.T., T.M., M.P. and T.L.-P.; validation, T.L.-P.; investigation, T.T., T.M., M.P. and T.L.-P.; resources, T.L.-P.; data curation, T.T., T.M., M.P. and T.L.-P.; writing—original draft preparation, T.T., T.M., M.P. and T.L.-P.; writing—review and editing, T.L.-P.; visualization, T.L.-P.; supervision, T.L.-P.; project administration, T.L.-P.; funding acquisition, T.L.-P. All authors have read and agreed to the published version of the manuscript.

**Funding:** T.L.P. and T.T. acknowledge the support provided by the Serbian Ministry of Science, Technological Development and Innovations (contract number: 451-03-136/2025-03/200017). T.M. acknowledges the support provided by Serbian Ministry of Science, Technological Development and Innovations (contract number: 0801–116/1). T.T. acknowledges the support provided by the Serbian Academy of Sciences and Arts (project no. F-49).

**Data Availability Statement:** No new data were created or analyzed in this study.

**Conflicts of Interest:** The authors declare no conflicts of interest.

## References

1. Li, X.; Shen, X.; Jiang, W.; Xi, Y.; Li, S. Comprehensive review of emerging contaminants: Detection technologies, environmental impact, and management strategies. *Ecotoxicol. Environ. Saf.* **2024**, *278*, 116420. https://doi.org/10.1016/j.ecoenv.2024.116420.
2. Picinini-Zambelli, J.; Garcia, A.L.H.; Da Silva, J. Emerging pollutants in the aquatic environments: A review of genotoxic impacts. *Mutat. Res.-Rev. Mutat. Res.* **2025**, *795*, 108519. https://doi.org/10.1016/j.mrrev.2024.108519.
3. Saha, R.; Dutta, S.M. Pesticides' mode of action on aquatic life. *Toxicol. Rep.* **2024**, *13*, 101780. https://doi.org/10.1016/j.toxrep.2024.101780.
4. Knapik, L.F.O.; Ramsdorf, W. Ecotoxicity of malathion pesticide and its genotoxic effects over the biomarker comet assay in Daphnia magna. *Environ. Monit. Assess.* **2020**, *192*, 264. https://doi.org/10.1007/s10661-020-8235-0.
5. Lu, X.W.; Dang, Z.; Yang, C. Preliminary investigation of chloramphenicol in fish, water and sediment from freshwater aquaculture pond. *Int. J. Environ. Sci. Technol.* **2009**, *6*, 597–604. https://doi.org/10.1007/BF03326100.
6. Zhang, T.; Jin, H. Aquatic toxicity of acetonitrile and its water quality criteria for the protection of aquatic life in China. *Int. J. Environ. Pollut.* **2001**, *15*, 568–575. https://doi.org/10.1504/IJEP.2001.004933.
7. Selvanathan, J.; Vincent, S.; Nirmala, A. Histopathology changes in freshwater fish *Clarias batrachus* (Linn.) exposed to mercury and cadmium. *Int. J. Life Sci. Pharma Res.* **2013**, *3*, 11–21.

8. Aib, H.; Parvez, M.S.; Czédli, H.M. Pharmaceuticals and Microplastics in Aquatic Environments: A Comprehensive Review of Pathways and Distribution, Toxicological and Ecological Effects. *Int. J. Environ. Res. Public Health* **2025**, *22*, 799. https://doi.org/10.3390/ijerph22050799.
9. da Cunha Neto, A.R.; da Silva, I.G.; Calvelli, J.V.B.; Martins, G.E.C.; Carvalho, M.; Barbosa, S. Toxicity of Heavy Metals that Affect Germination, Development and Cell Cycle of *Allium cepa* L. *Bull. Environ. Contam. Toxicol.* **2023**, *111*, 22. https://doi.org/10.1007/s00128-023-03775-9.
10. Galir, A.; Špoljarić Maronić, D.; Stević, F.; Žuna Pfeiffer, T.; Prašnikar, F.; Bek, N.; Penava, E.; Križevac, P. Effects of Azithromycin on the Functioning of the Food Web in Freshwater Plankton. *J. Xenobiotics* **2025**, *15*, 145. https://doi.org/10.3390/jox15050145.
11. Hama Aziz, K.H.; Mustafa, F.S.; Omer, K.M.; Hama, S.; Hamarawf, R.F.; Rahman, K.O. Heavy metal pollution in the aquatic environment: Efficient and low-cost removal approaches to eliminate their toxicity: A review. *RSC Adv.* **2023**, *13*, 17595–17610. https://doi.org/10.1039/D3RA00723E.
12. Branco, G.S.; Moreira, R.G.; Borella, M.I.; Camargo, M.d.P.; Muñoz-Peñuela, M.; Gomes, A.D.O.; Tolussi, C.E. Nonsteroidal anti-inflammatory drugs act as endocrine disruptors in *Astyanax lacustris* (Teleostei: Characidae) reproduction: An ex vivo approach. *Aquat. Toxicol.* **2021**, *232*, 105767. https://doi.org/10.1016/j.aquatox.2021.105767.
13. Lasagna, M.; Ventura, C.; Hielpos, M.S.; Mardirosian, M.N.; Martín, G.; Miret, N.; Randi, A.; Núñez, M.; Cocca, C. Endocrine disruptor chlorpyrifos promotes migration, invasion, and stemness phenotype in 3D cultures of breast cancer cells and induces a wide range of pathways involved in cancer progression. *Environ. Res.* **2022**, *204*, 111989. https://doi.org/10.1016/j.envres.2021.111989.
14. Wang, A.; Liu, Y.; Yan, Y.; Jiang, Y.; Shi, S.; Wang, J.; Qiao, K.; Yang, L.; Wang, S.; Li, S.; et al. Chlorpyrifos Influences Tadpole Development by Disrupting Thyroid Hormone Signaling Pathways. *Environ. Sci. Technol.* **2025**, *59*, 142–151. https://doi.org/10.1021/acs.est.4c07890.
15. Singh, R.; Wang, L.; Ostrikov, K.; Huang, J. Designing Carbon-Based Porous Materials for Carbon Dioxide Capture. *Adv. Mater. Interfaces* **2024**, *11*, 2202290. https://doi.org/10.1002/admi.202202290.
16. Huang, Y.; Luo, Y.; Liu, Z.; Xie, X.; Xue, M.; Gao, B. Engineering carbon materials for organic pollutant removal via adsorption and photodegradation: A review. *Sep. Purif. Technol.* **2025**, *359*, 130872. https://doi.org/10.1016/j.seppur.2024.130872.
17. Medeiros, D.C.C.d.S.; Chelme-Ayala, P.; Benally, C.; Al-Anzi, B.S.; Gamal El-Din, M. Review on carbon-based adsorbents from organic feedstocks for removal of organic contaminants from oil and gas industry process water: Production, adsorption performance and research gaps. *J. Environ. Manag.* **2022**, *320*, 115739. https://doi.org/10.1016/j.jenvman.2022.115739.
18. Lazarević-Pašti, T.; Jocić, A.; Milanković, V.; Tasić, T.; Batalović, K.; Breitenbach, S.; Unterweger, C.; Fürst, C.; Pašti, I.A. Investigating the Adsorption Kinetics of Dimethoate, Malathion and Chlorpyrifos on Cellulose-Derived Activated Carbons: Understanding the Influence of Physicochemical Properties. *C* **2023**, *9*, 103. https://doi.org/10.3390/c9040103.
19. Hashemzadeh, F.; Ariannezhad, M.; Derakhshandeh, S.H. Sustainable removal of tetracycline and paracetamol from water using magnetic activated carbon derived from pine fruit waste. *Sci. Rep.* **2024**, *14*, 16346. https://doi.org/10.1038/s41598-024-65656-3.
20. Sajid, M.; Bari, S.; Saif Ur Rehman, M.; Ashfaq, M.; Guoliang, Y.; Mustafa, G. Adsorption characteristics of paracetamol removal onto activated carbon prepared from Cannabis sativum Hemp. *Alex. Eng. J.* **2022**, *61*, 7203–7212. https://doi.org/10.1016/j.aej.2021.12.060.
21. Albatrni, H.; Qiblawey, H. A Novel Activated Carbon-Based Composite for Enhanced Mercury Removal. *Water* **2025**, *17*, 2035.
22. Dou, Z.; Wang, Y.; Liu, Y.; Zhao, Y.; Huang, R. Enhanced adsorption of gaseous mercury on activated carbon by a novel clean modification method. *Sep. Purif. Technol.* **2023**, *308*, 122885. https://doi.org/10.1016/j.seppur.2022.122885.
23. Abioye, S.O.; Majooni, Y.; Moayedi, M.; Rezvani, H.; Kapadia, M.; Yousefi, N. Graphene-based nanomaterials for the removal of emerging contaminants of concern from water and their potential adaptation for point-of-use applications. *Chemosphere* **2024**, *355*, 141728. https://doi.org/10.1016/j.chemosphere.2024.141728.
24. Lazarević-Pašti, T.; Anićijević, V.; Baljozović, M.; Anićijević, D.V.; Gutić, S.; Vasić, V.; Skorodumova, N.V.; Pašti, I.A. The impact of the structure of graphene-based materials on the removal of organophosphorus pesticides from water. *Environ. Sci. Nano* **2018**, *5*, 1482–1494. https://doi.org/10.1039/C8EN00171E.
25. Sarkar, B.; Mandal, S.; Tsang, Y.F.; Kumar, P.; Kim, K.-H.; Ok, Y.S. Designer carbon nanotubes for contaminant removal in water and wastewater: A critical review. *Sci. Total Environ.* **2018**, *612*, 561–581. https://doi.org/10.1016/j.scitotenv.2017.08.132.

26. Duarte, M.P.; Silva, R.C.F.; Medeiros, T.P.V.d.; Ardisson, J.D.; Cotta, A.A.C.; Naccache, R.; Teixeira, A.P.d.C. Carbon nanotubes derived from waste cooking oil for the removal of emerging contaminants. *New J. Chem.* **2022**, *46*, 11315–11328. https://doi.org/10.1039/D2NJ01669A.
27. Trivedi, Y.; Sharma, M.; Mishra, R.K.; Sharma, A.; Joshi, J.; Gupta, A.B.; Achintya, B.; Shah, K.; Vuppaladadiyamd, A.K. Biochar potential for pollutant removal during wastewater treatment: A comprehensive review of separation mechanisms, technological integration, and process analysis. *Desalination* **2025**, *600*, 118509. https://doi.org/10.1016/j.desal.2024.118509.
28. Zlatković, M.; Kurtić, R.; Pašti, I.A.; Tasić, T.; Milanković, V.; Potkonjak, N.; Unterweger, C.; Lazarević-Pašti, T. Application of Carbon Materials Derived from Nocino Walnut Liqueur Pomace Residue for Chlorpyrifos Removal from Water. *Materials* **2025**, *18*, 3072. https://doi.org/10.3390/ma18133072.
29. Jia, L.; Fan, B.-g.; Yao, Y.-x.; Han, F.; Huo, R.-p.; Zhao, C.-w.; Jin, Y. Study on the Elemental Mercury Adsorption Characteristics and Mechanism of Iron-Based Modified Biochar Materials. *Energy Fuels* **2018**, *32*, 12554–12566. https://doi.org/10.1021/acs.energyfuels.8b02890.
30. Wang, H.; Duan, R.; Zhou, X.; Wang, J.; Liu, Y.; Xu, R.; Liao, Z. Efficient removal of mercury and chromium from wastewater via biochar fabricated with steel slag: Performance and mechanisms. *Front. Bioeng. Biotechnol.* **2022**, *10*, 961907. https://doi.org/10.3389/fbioe.2022.961907.
31. Jacob, M.M.; Ponnuchamy, M.; Kapoor, A.; Sivaraman, P. Achieving up to 95% removal efficiency of chlorpyrifos pesticide using sugarcane bagasse-based biochar alginate beads in a continuous fixed-bed adsorption column. *Environ. Res.* **2025**, *269*, 120902. https://doi.org/10.1016/j.envres.2025.120902.
32. Celso Gonçalves, A.; Zimmermann, J.; Schwantes, D.; Tarley, C.R.T.; Conradi Junior, E.; Henrique Dias de Oliveira, V.; Campagnolo, M.A.; Ziemer, G.L. Renewable Eco-Friendly Activated Biochar from Tobacco: Kinetic, Equilibrium and Thermodynamics Studies for Chlorpyrifos Removal. *Sep. Sci. Technol.* **2022**, *57*, 159–179. https://doi.org/10.1080/01496395.2021.1890776.
33. Baylan, N.; Van Eygen, G.; Van der Bruggen, B. Ionic liquid membranes for the separation of phenols, metals, drugs and other compounds from aqueous media: A review of new developments. *J. Water Process Eng.* **2024**, *68*, 106576. https://doi.org/10.1016/j.jwpe.2024.106576.
34. Toledo Hijo, A.A.C.; Alves, C.; Farias, F.O.; Peixoto, V.S.; Meirelles, A.J.A.; Santos, G.H.F.; Maximo, G.J. Ionic liquids and deep eutectic solvents as sustainable alternatives for efficient extraction of phenolic compounds from mate leaves. *Food Res. Int.* **2022**, *157*, 111194. https://doi.org/10.1016/j.foodres.2022.111194.
35. Cheshmekhezr, S.; Rothee, S.R.; Nazaripour, M.; Rahman, A.; Heidari, H.; Masrura, S.U.; Khan, E. Exploring ionic liquids and deep eutectic solvents for emerging contaminant removal from water and wastewater. *NPJ Mater. Sustain.* **2024**, *2*, 38. https://doi.org/10.1038/s44296-024-00042-8.
36. Stanton Ribeiro, M.; Zanatta, M.; Corvo, M.C. Ionic liquids and biomass as carbon precursors: Synergistically answering a call for $CO_2$ capture and conversion. *Fuel* **2022**, *327*, 125164. https://doi.org/10.1016/j.fuel.2022.125164.
37. He, X.; Zhu, J.; Wang, H.; Zhou, M.; Zhang, S. Surface Functionalization of Activated Carbon with Phosphonium Ionic Liquid for $CO_2$ Adsorption. *Coatings* **2019**, *9*, 590. https://doi.org/10.3390/coatings9090590.
38. Ayyildiz, M.; Hetze, K.; Schutjajew, K.; Poudel, P.; Paulus, R.M.; Schacher, F.H.; Dellith, J.; Schubert, U.S.; Oschatz, M. Understanding the Interplay Between Pore Structure and Ionic Liquid Interaction on the Gas Uptake of Microporous Carbons. *Small* **2025**, *21*, e01928. https://doi.org/10.1002/smll.202501928.
39. Wei, L.; Wang, L.; Cui, Z.; Liu, Y.; Du, A. Multifunctional Applications of Ionic Liquids in Polymer Materials: A Brief Review. *Molecules* **2023**, *28*, 3836. https://doi.org/10.3390/molecules28093836.
40. Matuszek, K.; Piper, S.L.; Brzęczek-Szafran, A.; Roy, B.; Saher, S.; Pringle, J.M.; MacFarlane, D.R. Unexpected Energy Applications of Ionic Liquids. *Adv. Mater.* **2024**, *36*, 2313023. https://doi.org/10.1002/adma.202313023.
41. Salas, R.; Villa, R.; Velasco, F.; Cirujano, F.G.; Nieto, S.; Martin, N.; Garcia-Verdugo, E.; Dupont, J.; Lozano, P. Ionic liquids in polymer technology. *Green Chem.* **2025**, *27*, 1620–1651. https://doi.org/10.1039/D4GC05445H.
42. Zhang, S.; Dokko, K.; Watanabe, M. Carbon materialization of ionic liquids: From solvents to materials. *Mater. Horiz.* **2015**, *2*, 168–197. https://doi.org/10.1039/C4MH00141A.
43. Maiyelvaganan, K.R.; Kamalakannan, S.; Prakash, M. Adsorption of ionic liquids on carbonaceous surfaces: The effect of curvature on selective anion···π and cation···π interactions. *Appl. Surf. Sci.* **2019**, *495*, 143538. https://doi.org/10.1016/j.apsusc.2019.143538.

44. Wang, W.; Zhao, N.; Zhao, K.; Zhang, M.; Pang, K.; Zhang, Y.; Yuan, J. Multi-heteroatom-doped porous carbon electrodes from 3D printing and conformal carbonization of ionic liquids for electrocatalytic $CO_2$ conversion into syngas. *Commun. Chem.* **2025**, *8*, 121. https://doi.org/10.1038/s42004-025-01514-1.
45. Ab Rahim, A.H.; Yunus, N.M.; Bustam, M.A. Ionic Liquids Hybridization for Carbon Dioxide Capture: A Review. *Molecules* **2023**, *28*, 7091. https://doi.org/10.3390/molecules28207091.
46. Hussain, S.; Ali, A.; Foorginezhad, S.; Chen, Y.; Ji, X. A comprehensive review on ionic liquids and ionic hybrid materials for $CO_2$ separation. *Sep. Purif. Technol.* **2025**, *360*, 130997. https://doi.org/10.1016/j.seppur.2024.130997.
47. Zhang, C.; Qu, P.; Zhou, M.; Qian, L.; Bai, T.; Jin, J.; Xin, B. Ionic Liquids as Promisingly Multi-Functional Participants for Electrocatalyst of Water Splitting: A Review. *Molecules* **2023**, *28*, 3051. https://doi.org/10.3390/molecules28073051.
48. Anuchi, S.O.; Campbell, K.L.S.; Hallett, J.P. Effects of the Ionic Liquid Structure on Porosity of Lignin-Derived Carbon Materials. *ACS Sustain. Chem. Eng.* **2023**, *11*, 15228–15241. https://doi.org/10.1021/acssuschemeng.3c03035.
49. Zafar, A.; Matuszek, K.; MacFarlane, D.R.; Zhang, X. Recent progress and future perspectives of ionic liquid-based carbon dioxide capture and conversion. *Green Energy Environ.* **2025**, *10*, 1097–1129. https://doi.org/10.1016/j.gee.2024.10.002.
50. Guo, Q.; Chen, C.; Xing, F.; Shi, W.; Meng, J.; Wan, H.; Guan, G. Constructing Hierarchically Porous N-Doped Carbons Derived from Poly(ionic liquids) with the Multifunctional Fe-Based Template for $CO_2$ Adsorption. *ACS Omega* **2021**, *6*, 7186–7198. https://doi.org/10.1021/acsomega.1c00419.
51. Kiciński, W.; Dyjak, S. Nitrogen-Doped Carbons Derived from Imidazole-Based Cross-Linked Porous Organic Polymers. *Molecules* **2021**, *26*, 668. https://doi.org/10.3390/molecules26030668.
52. Aldroubi, S.; Larhrib, B.; Larbi, L.; Malham, I.B.; Ghimbeu, C.M.; Monconduit, L.; Mehdi, A.; Brun, N. Tailored imidazolium tetraphenylborate salts for the design of boron, nitrogen co-doped carbon materials as high-performance anodes for fast-rate monovalent ion batteries. *J. Mater. Chem. A* **2023**, *11*, 16755–16766. https://doi.org/10.1039/D3TA02611F.
53. Severin, A.A.; Rauber, D.; Pachoula, S.; Philippi, F.; Radev, I.; Holtsch, A.; Müller, F.; Baumgärtner, M.; Hempelmann, R.; Kay, C.W.M. P-containing coated carbons from phosphonium ionic liquids as catalyst supports for fuel cell applications. *Sustain. Energy Fuels* **2023**, *7*, 752–762. https://doi.org/10.1039/D2SE01332K.
54. Zhang, B.; Petcher, S.; Gao, H.; Yan, P.; Cai, D.; Fleming, G.; Parker, D.J.; Chong, S.Y.; Hasell, T. Magnetic sulfur-doped carbons for mercury adsorption. *J. Colloid Interface Sci.* **2021**, *603*, 728–737. https://doi.org/10.1016/j.jcis.2021.06.129.
55. Saha, D.; Richards, C.P.; Haines, R.G.; D'Alessandro, N.D.; Kienbaum, M.J.; Griffaton, C.A. Soft-Templating of Sulfur and Iron Dual-Doped Mesoporous Carbons: Lead Adsorption in Mixtures. *Molecules* **2020**, *25*, 403. https://doi.org/10.3390/molecules25020403.
56. Austin, D.; Jahan, K.; Feng, X.; Carney, J.; Hensley, D.K.; Chen, J.; Altidor, B.E.; Guo, Z.; Michaelis, E.; Kebaso, M.K.; et al. Sulfur functionalized biocarbon sorbents for low-concentration mercury isolation. *Dalton Trans.* **2024**, *53*, 2098–2107. https://doi.org/10.1039/D3DT02625F.
57. Pancielejko, A.; Kroczewska-Gnatowska, M.; Mazierski, P.; Łuczak, J.; Zaleska-Medynska, A. The effect of ionic liquids on the surface and photocatalytic properties of semiconducting materials. *Chem. Eng. J.* **2024**, *498*, 155274. https://doi.org/10.1016/j.cej.2024.155274.
58. García-Suárez, E.J.; Menéndez-Vázquez, C.; García, A.B. Chemical stability of choline-based ionic liquids supported on carbon materials. *J. Mol. Liq.* **2012**, *169*, 37–42. https://doi.org/10.1016/j.molliq.2012.02.022.
59. Latini, G.; Signorile, M.; Rosso, F.; Fin, A.; d'Amora, M.; Giordani, S.; Pirri, F.; Crocellà, V.; Bordiga, S.; Bocchini, S. Efficient and reversible $CO_2$ capture in bio-based ionic liquids solutions. *J. $CO_2$ Util.* **2022**, *55*, 101815. https://doi.org/10.1016/j.jcou.2021.101815.
60. Ye, D.; Leung, K.C.; Niu, W.; Duan, M.; Li, J.; Ho, P.-L.; Szalay, D.; Wu, T.-S.; Soo, Y.-L.; Wu, S.; et al. Active nitrogen sites on nitrogen doped carbon for highly efficient associative ammonia decomposition. *iScience* **2024**, *27*, 110571. https://doi.org/10.1016/j.isci.2024.110571.
61. Guo, Z.; Hermesdorf, M.; Chen, Y.; Feng, P.; Lu, Y.; Oschatz, M.; Leistenschneider, D. Impact of nitrogen functionalization and porosity on the electrosorption of ionic liquids on templated porous carbons. *Electrochim. Acta* **2025**, *518*, 145751. https://doi.org/10.1016/j.electacta.2025.145751.
62. Li, X.-F.; Lian, K.-Y.; Liu, L.; Wu, Y.; Qiu, Q.; Jiang, J.; Deng, M.; Luo, Y. Unraveling the formation mechanism of graphitic nitrogen-doping in thermally treated graphene with ammonia. *Sci. Rep.* **2016**, *6*, 23495. https://doi.org/10.1038/srep23495.
63. Zhou, J.; Yang, P.; Kots, P.A.; Cohen, M.; Chen, Y.; Quinn, C.M.; de Mello, M.D.; Anibal Boscoboinik, J.; Shaw, W.J.; Caratzoulas, S.; et al. Tuning the reactivity of carbon surfaces with oxygen-containing functional groups. *Nat. Commun.* **2023**, *14*, 2293. https://doi.org/10.1038/s41467-023-37962-3.

64. Cao, S.; Zhao, Y.; Cao, Y.; Li, Y.; Tan, H.; Wang, H. Ionic liquid-assisted biomass-derived N, S-doped carbon dots with enhanced corrosion inhibition. *Sci. Rep.* **2025**, *15*, 23056. https://doi.org/10.1038/s41598-025-04444-z.
65. Quoie, G.D.S., Jr.; Jiao, M.; Lászlód, K.; Wang, Y. Progress Made in Non-Metallic-Doped Materials for Electrocatalytic Reduction in Ammonia Production. *Materials* **2024**, *17*, 2419. https://doi.org/10.3390/ma17102419.
66. Yang, S.Y.; Bai, B.C.; Kim, Y.R. Effective Surface Structure Changes and Characteristics of Activated Carbon with the Simple Introduction of Oxygen Functional Groups by Using Radiation Energy. *Surfaces* **2024**, *7*, 12–25. https://doi.org/10.3390/surfaces7010002.
67. Wang, B.; Lan, J.; Bo, C.; Gong, B.; Ou, J. Adsorption of heavy metal onto biomass-derived activated carbon: Review. *RSC Adv.* **2023**, *13*, 4275–4302. https://doi.org/10.1039/D2RA07911A.
68. Jaramillo-Fierro, X.; Cuenca, G. Theoretical and Experimental Analysis of Hydroxyl and Epoxy Group Effects on Graphene Oxide Properties. *Nanomaterials* **2024**, *14*, 714. https://doi.org/10.3390/nano14080714.
69. Rahim, H.U.; Allevato, E.; Stazi, S.R. Sulfur-functionalized biochar: Synthesis, characterization, and utilization for contaminated soil and water remediation-a review. *J. Environ. Manag.* **2024**, *370*, 122670. https://doi.org/10.1016/j.jenvman.2024.122670.
70. Wu, J.; Jing, R.; Wu, Y.; Li, J.; Guo, C.; Jiang, C.; Zeng, K.; Yang, R. Ionic liquid derived heteroatom-adaptive porous carbon electrode Harness high-performance supercapacitors: Momentous roles of microstructure and self-doped bridge active sites. *Carbon* **2025**, *244*, 120679. https://doi.org/10.1016/j.carbon.2025.120679.
71. Bengtsson, A.; Hecht, P.; Sommertune, J.; Ek, M.; Sedin, M.; Sjöholm, E. Carbon Fibers from Lignin–Cellulose Precursors: Effect of Carbonization Conditions. *ACS Sustain. Chem. Eng.* **2020**, *8*, 6826–6833. https://doi.org/10.1021/acssuschemeng.0c01734.
72. Ovejero-Pérez, A.; Nakasu, P.Y.S.; Hopson, C.; Costa, J.M.; Hallett, J.P. Challenges and opportunities on the utilisation of ionic liquid for biomass pretreatment and valorisation. *NPJ Mater. Sustain.* **2024**, *2*, 7. https://doi.org/10.1038/s44296-024-00015-x.
73. Atashnezhad, A.; Scott, J.; Al Dushaishi, M.F. Environmental Implications of Ionic Liquid and Deep Eutectic Solvent in Geothermal Application: Comparing Traditional and New Approach Methods. *ACS Sustain. Chem. Eng.* **2024**, *12*, 14684–14693. https://doi.org/10.1021/acssuschemeng.4c04606.
74. Albeladi, N.; Blankenship, L.S.; Mokaya, R. Ultra-high surface area ionic-liquid-derived carbons that meet both gravimetric and volumetric methane storage targets. *Energy Environ. Sci.* **2024**, *17*, 3060–3076. https://doi.org/10.1039/D3EE03957A.
75. Rodriguez-Reartes, S.B.; Llovell, F. Characterizing the Potential of Phosphonium-Based Ionic Liquids for $CO_2$ Capture via Multiscale Modeling. *Ind. Eng. Chem. Res.* **2025**, *64*, 17878–17891. https://doi.org/10.1021/acs.iecr.5c01361.
76. Zhang, S.; Miran, M.S.; Ikoma, A.; Dokko, K.; Watanabe, M. Protic Ionic Liquids and Salts as Versatile Carbon Precursors. *J. Am. Chem. Soc.* **2014**, *136*, 1690–1693. https://doi.org/10.1021/ja411981c.
77. França, J.M.P.; Nieto de Castro, C.A.; Pádua, A.A.H. Molecular interactions and thermal transport in ionic liquids with carbon nanomaterials. *Phys. Chem. Chem. Phys.* **2017**, *19*, 17075–17087. https://doi.org/10.1039/C7CP01952A.
78. Pensado, A.S.; Malberg, F.; Gomes, M.F.C.; Pádua, A.A.H.; Fernández, J.; Kirchner, B. Interactions and structure of ionic liquids on graphene and carbon nanotubes surfaces. *RSC Adv.* **2014**, *4*, 18017–18024. https://doi.org/10.1039/C4RA02059F.
79. Shakourian-Fard, M.; Jamshidi, Z.; Bayat, A.; Kamath, G. Meta-Hybrid Density Functional Theory Study of Adsorption of Imidazolium- and Ammonium-Based Ionic Liquids on Graphene Sheet. *J. Phys. Chem. C* **2015**, *119*, 7095–7108. https://doi.org/10.1021/jp512020q.
80. Moosavi, F.; Razmkhah, M. Structural View of Hydrophobic Ionic Liquid on Graphene: Comparing Static and Ab Initio Computer Simulations. *ECS J. Solid State Sci. Technol.* **2015**, *4*, M77. https://doi.org/10.1149/2.0091512jss.
81. Ruzanov, A.; Lembinen, M.; Ers, H.; García de la Vega, J.M.; Lage-Estebanez, I.; Lust, E.; Ivaništšev, V.B. Density Functional Theory Study of Ionic Liquid Adsorption on Circumcoronene Shaped Graphene. *J. Phys. Chem. C* **2018**, *122*, 2624–2631. https://doi.org/10.1021/acs.jpcc.7b12156.
82. Zambare, R.; Song, X.; Bhuvana, S.; Antony Prince, J.S.; Nemade, P. Ultrafast Dye Removal Using Ionic Liquid–Graphene Oxide Sponge. *ACS Sustain. Chem. Eng.* **2017**, *5*, 6026–6035. https://doi.org/10.1021/acssuschemeng.7b00867.
83. Lawal, I.A.; Lawal, M.M.; Akpotu, S.O.; Okoro, H.K.; Klink, M.; Ndungu, P. Noncovalent Graphene Oxide Functionalized with Ionic Liquid: Theoretical, Isotherm, Kinetics, and Regeneration Studies on the Adsorption of Pharmaceuticals. *Ind. Eng. Chem. Res.* **2020**, *59*, 4945–4957. https://doi.org/10.1021/acs.iecr.9b06634.
84. Verma, C.; Ebenso, E.E. Ionic liquid-mediated functionalization of graphene-based materials for versatile applications: A review. *Graphene Technol.* **2019**, *4*, 1–15. https://doi.org/10.1007/s41127-018-0023-z.
85. Fatima, S.S.; Borhan, A.; Ayoub, M.; Ghani, N.A. $CO_2$ Adsorption Performance on Surface-Functionalized Activated Carbon Impregnated with Pyrrolidinium-Based Ionic Liquid. *Processes* **2022**, *10*, 2372. https://doi.org/10.3390/pr10112372.

86. Eyckens, D.J.; Servinis, L.; Scheffler, C.; Wölfel, E.; Demir, B.; Walsh, T.R.; Henderson, L.C. Synergistic interfacial effects of ionic liquids as sizing agents and surface modified carbon fibers. *J. Mater. Chem. A* **2018**, *6*, 4504–4514. https://doi.org/10.1039/C7TA10516A.
87. Ghafoor, B.; Schrekker, H.S.; Amico, S.C. Multifunctional Characteristics of Carbon Fibers Modified with Imidazolium Ionic Liquids. *Molecules* **2022**, *27*, 7001. https://doi.org/10.3390/molecules27207001.
88. Wang, D.; Zhao, L.; Cui, Y.; Tong, Y.; Li, X.; Liu, P.; Hu, H.; Nan, J.; Wu, W.; Xu, H.; et al. Intermolecular π-π stacking of oligomeric naphthalene cathodes facilitate high performance aluminum ion battery. *Chem. Eng. J.* **2024**, *482*, 148806. https://doi.org/10.1016/j.cej.2024.148806.
89. Ahmad, I.; Li, H.; Ahmed, S.B.; Alotaibi, M.T.; Li, G. Shedding light on unprecedented spatial confinement of metal clusters by metal/covalent organic frameworks for photocatalysis. *Appl. Phys. Rev.* **2025**, *12*, 041327. https://doi.org/10.1063/5.0285638.
90. Leonhardi, J.; Schnarkowski, B.; Mehdorn, M.; Höhn, A.K.; Niebisch, S.; Plum, P.; Seehofer, D.; Tiepolt, S.; Denecke, T.; Meyer, H.J. Diagnostic Accuracy and Reliability of CT-based Node-RADS for Esophageal Cancer. *In vivo* **2025**, *39*, 353–359. https://doi.org/10.21873/invivo.13835.
91. Zhou, X.; Zhang, Y.; Huang, Z.; Lu, D.; Zhu, A.; Shi, G. Ionic liquids modified graphene oxide composites: A high efficient adsorbent for phthalates from aqueous solution. *Sci. Rep.* **2016**, *6*, 38417. https://doi.org/10.1038/srep38417.
92. Wojsławski, J.; Białk-Bielińska, A.; Paszkiewicz, M.; Toński, M.; Stepnowski, P.; Dołżonek, J. Evaluation of the sorption mechanism of ionic liquids onto multi-walled carbon nanotubes. *Chemosphere* **2018**, *190*, 280–286. https://doi.org/10.1016/j.chemosphere.2017.09.043.
93. Costa, R.; Pereira, C.M.; Silva, A.F. Insight on the effect of surface modification by carbon materials on the Ionic Liquid Electric Double Layer Charge Storage properties. *Electrochim. Acta* **2015**, *176*, 880–886. https://doi.org/10.1016/j.electacta.2015.06.142.
94. Zhang, W.-H.; He, P.-P.; Wu, S.; Xu, J.; Li, Y.; Zhang, G.; Wei, X.-Y. Graphene oxide grafted hydroxyl-functionalized ionic liquid: A highly efficient catalyst for cycloaddition of $CO_2$ with epoxides. *Appl. Catal. A: Gen.* **2016**, *509*, 111–117. https://doi.org/10.1016/j.apcata.2015.10.038.
95. Krishna Kumar, A.S.; Jiang, S.-J.; Tseng, W.-L. Effective adsorption of chromium(vi)/Cr(iii) from aqueous solution using ionic liquid functionalized multiwalled carbon nanotubes as a super sorbent. *J. Mater. Chem. A* **2015**, *3*, 7044–7057. https://doi.org/10.1039/C4TA06948J.
96. Li, L.; Luo, C.; Li, X.; Duan, H.; Wang, X. Preparation of magnetic ionic liquid/chitosan/graphene oxide composite and application for water treatment. *Int. J. Biol. Macromol.* **2014**, *66*, 172–178. https://doi.org/10.1016/j.ijbiomac.2014.02.031.
97. Kumar, A.S.K.; Rajesh, N. Exploring the interesting interaction between graphene oxide, Aliquat-336 (a room temperature ionic liquid) and chromium(vi) for wastewater treatment. *RSC Adv.* **2013**, *3*, 2697–2709. https://doi.org/10.1039/C2RA22627H.
98. Deng, F.; Liang, J.; Yang, G.; Huang, Q.; Dou, J.; Chen, J.; Wen, Y.; Liu, M.; Zhang, X.; Wei, Y. Direct generation of poly(ionic liquids) on mesoporous carbon via Diels–Alder and multicomponent reactions for ultrafast adsorptive removal anionic organic dye with high efficiency. *J. Environ. Chem. Eng.* **2021**, *9*, 104872. https://doi.org/10.1016/j.jece.2020.104872.
99. Roy, S.; Ahmaruzzaman, M. Ionic liquid based composites: A versatile materials for remediation of aqueous environmental contaminants. *J. Environ. Manag.* **2022**, *315*, 115089. https://doi.org/10.1016/j.jenvman.2022.115089.
100. Zhao, W.; Tang, Y.; Xi, J.; Kong, J. Functionalized graphene sheets with poly(ionic liquid)s and high adsorption capacity of anionic dyes. *Appl. Surf. Sci.* **2015**, *326*, 276–284. https://doi.org/10.1016/j.apsusc.2014.11.069.
101. Zhang, X.; Peng, Y.; Liu, F.; Peng, Q.; Wan, L.; Cheng, J.; He, J. Improvement of tetracycline removal using amino acid ionic liquid modified magnetic biochar based on theoretical design. *Sep. Purif. Technol.* **2025**, *357*, 130187. https://doi.org/10.1016/j.seppur.2024.130187.
102. Cardoso, A.T.; Domínguez-Rodríguez, G.; Cifuentes, A.; Lanças, F.M. Ionic liquid-grafted aminosilica-graphene oxide sorbent for efficient microextraction by packed sorbent of multiclass pesticides in wine. *Adv. Sample Prep.* **2025**, *16*, 100217. https://doi.org/10.1016/j.sampre.2025.100217.
103. Zambare, R.S.; Song, X.; Bhuvana, S.; Tang, C.Y.; Prince, J.S.A.; Nemade, P.R. Ionic Liquid-Reduced Graphene Oxide Membrane with Enhanced Stability for Water Purification. *ACS Appl. Mater. Interfaces* **2022**, *14*, 43339–43353. https://doi.org/10.1021/acsami.2c12488.
104. Krishna, R.H.; Chandraprabha, M.N.; Samrat, K.; Krishna Murthy, T.P.; Manjunatha, C.; Kumar, S.G. Carbon nanotubes and graphene-based materials for adsorptive removal of metal ions—A review on surface functionalization and related adsorption mechanism. *Appl. Surf. Sci. Adv.* **2023**, *16*, 100431. https://doi.org/10.1016/j.apsadv.2023.100431.
105. Lee, A.; Choe, J.K.; Zoh, K.D.; Lee, C.; Choi, Y. Development of ionic-liquid-impregnated activated carbon for sorptive removal of PFAS in drinking water treatment. *Chemosphere* **2024**, *355*, 141872. https://doi.org/10.1016/j.chemosphere.2024.141872.

106. Lee, A.; Kim, J.; Choe, J.K.; Choi, Y. Ionic liquid-grafted activated carbon for selective removal of PFAS by adsorption in drinking water. *Chemosphere* **2024**, *369*, 143902. https://doi.org/10.1016/j.chemosphere.2024.143902.
107. Wang, H.; Wei, Y. Magnetic graphene oxide modified by chloride imidazole ionic liquid for the high-efficiency adsorption of anionic dyes. *RSC Adv.* **2017**, *7*, 9079–9089. https://doi.org/10.1039/C6RA27530C.
108. Barik, B.; Kumar, A.; Nayak, P.S.; Achary, L.S.K.; Rout, L.; Dash, P. Ionic liquid assisted mesoporous silica-graphene oxide nanocomposite synthesis and its application for removal of heavy metal ions from water. *Mater. Chem. Phys.* **2020**, *239*, 122028. https://doi.org/10.1016/j.matchemphys.2019.122028.
109. Erto, A.; Silvestre-Albero, A.; Silvestre-Albero, J.; Rodríguez-Reinoso, F.; Balsamo, M.; Lancia, A.; Montagnaro, F. Carbon-supported ionic liquids as innovative adsorbents for $CO_2$ separation from synthetic flue-gas. *J. Colloid Interface Sci.* **2015**, *448*, 41–50. https://doi.org/10.1016/j.jcis.2015.01.089.
110. Sun, W.; Li, L.; Luo, C.; Fan, L. Synthesis of magnetic graphene nanocomposites decorated with ionic liquids for fast lead ion removal. *Int. J. Biol. Macromol.* **2016**, *85*, 246–251. https://doi.org/10.1016/j.ijbiomac.2015.09.061.
111. Zhang, M.; Ma, X.; Li, J.; Huang, R.; Guo, L.; Zhang, X.; Fan, Y.; Xie, X.; Zeng, G. Enhanced removal of As(III) and As(V) from aqueous solution using ionic liquid-modified magnetic graphene oxide. *Chemosphere* **2019**, *234*, 196–203. https://doi.org/10.1016/j.chemosphere.2019.06.057.
112. Tong, G.; Lei, E.; Xu, Z.; Ma, C.; Li, W.; Liu, S. Preparation, Modification and Application of Carbon Materials Based on Ionic Liquids. *Prog. Chem.* **2019**, *31*, 1136–1147. https://doi.org/10.7536/PC181218.
113. Zhang, H.; Ling, Y.; Peng, Y.; Zhang, J.; Guan, S. Nitrogen-doped porous carbon materials derived from ionic liquids as electrode for supercapacitor. *Inorg. Chem. Commun.* **2020**, *115*, 107856. https://doi.org/10.1016/j.inoche.2020.107856.
114. Sun, L.; Yao, Y.; Zhou, Y.; Li, L.; Zhou, H.; Guo, M.; Liu, S.; Feng, C.; Qi, Z.; Gao, B. Solvent-Free Synthesis of N/S-Codoped Hierarchically Porous Carbon Materials from Protic Ionic Liquids for Temperature-Resistant, Flexible Supercapacitors. *ACS Sustain. Chem. Eng.* **2018**, *6*, 13494–13503. https://doi.org/10.1021/acssuschemeng.8b03528.
115. Zhao, Z.; Sun, Z.; Lv, W.; Sun, C.; Zhang, Z. Preparation of graphene/carbon nanotube-cellulose composites assisted by ionic liquids: A review. *Int. J. Biol. Macromol.* **2024**, *276*, 133927. https://doi.org/10.1016/j.ijbiomac.2024.133927.
116. Deng, X.; Lü, L.; Li, H.; Luo, F. The adsorption properties of Pb(II) and Cd(II) on functionalized graphene prepared by electrolysis method. *J. Hazard. Mater.* **2010**, *183*, 923–930. https://doi.org/10.1016/j.jhazmat.2010.07.117.
117. Jahanshahi, M.; Kowsari, E.; Haddadi-Asl, V.; Khoobi, M.; Bazri, B.; Aryafard, M.; Lee, J.H.; Kadumudi, F.B.; Talebian, S.; Kamaly, N.; et al. An innovative and eco-friendly modality for synthesis of highly fluorinated graphene by an acidic ionic liquid: Making of an efficacious vehicle for anti-cancer drug delivery. *Appl. Surf. Sci.* **2020**, *515*, 146071. https://doi.org/10.1016/j.apsusc.2020.146071.
118. Kowsari, E.; Ehsani, A.; Dashti Najafi, M. Electrosynthesis and pseudocapacitance performance of ionic liquid—Cr ($\eta^6$-$C_6H_5$) complex functionalized reduced graphene oxide/poly ortho aminophenol nanocomposite film. *J. Colloid Interface Sci.* **2017**, *504*, 507–513. https://doi.org/10.1016/j.jcis.2017.05.117.
119. Romann, T.; Anderson, E.; Pikma, P.; Tamme, H.; Möller, P.; Lust, E. Reactions at graphene|tetracyanoborate ionic liquid interface—New safety mechanisms for supercapacitors and batteries. *Electrochem. Commun.* **2017**, *74*, 38–41. https://doi.org/10.1016/j.elecom.2016.11.016.
120. Yan, Y.; Hao, X.-F.; Gao, L.-g.; Lin, S.-s.; Cui, N.; Li, Y.-h.; Hao, C.; Ma, T.-l.; Wang, H.-x. Highly accessible hierarchical porous carbon from a bi-functional ionic liquid bulky gel: High-performance electrochemical double layer capacitors. *J. Mater. Chem. A* **2019**, *7*, 25297–25304. https://doi.org/10.1039/C9TA07820G.
121. Verma, A.; Singh, V.V.; Pandey, L.K.; Upadhyay, S.; Thakare, V.B.; Shukla, P.K. Ionic liquid-carbon hybrid material for toxic gas removal: A sustainable approach for environmental cleanup. *Chem. Eng. J.* **2025**, *505*, 159785. https://doi.org/10.1016/j.cej.2025.159785.
122. Shu Hui, T.; Ahmad Zaini, M.A. Potassium hydroxide activation of activated carbon: A commentary. *Carbon Lett.* **2015**, *16*, 275–280. https://doi.org/10.5714/CL.2015.16.4.275.
123. Mbarki, F.; Selmi, T.; Kesraoui, A.; Seffen, M. Low-cost activated carbon preparation from Corn stigmata fibers chemically activated using $H_3PO_4$, $ZnCl_2$ and KOH: Study of methylene blue adsorption, stochastic isotherm and fractal kinetic. *Ind. Crops Prod.* **2022**, *178*, 114546. https://doi.org/10.1016/j.indcrop.2022.114546.
124. Bedia, J.; Peñas-Garzón, M.; Gómez-Avilés, A.; Rodriguez, J.J.; Belver, C. Review on Activated Carbons by Chemical Activation with $FeCl_3$. *C* **2020**, *6*, 21. https://doi.org/10.3390/c6020021.

125. Fan, M.; Shao, Y.; Wang, Y.; Sun, J.; He, H.; Jiang, Y.; Zhang, S.; Wang, Y.; Hu, X. Preparation of activated carbon with recycled $ZnCl_2$ for maximizing utilization efficiency of the activating agent and minimizing generation of liquid waste. *Chem. Eng. J.* **2024**, *500*, 157278. https://doi.org/10.1016/j.cej.2024.157278.
126. Karimi, B.; Ma'manib, L.; Karimi, H.; Hossini, H. Ionic liquid modified magnetic nanoparticles-graphene hybrid ($Fe_3O_4$@GO-IL) for the removal of ibuprofen and penicillin G from aqueous solutions. *Desalination Water Treat.* **2020**, *208*, 355–366. https://doi.org/10.5004/dwt.2020.26473.
127. Peng, Y.; Zhang, X.; Liu, F.; Zhen, D.; Jiao, Y.; Peng, Q. Metal-based ionic liquid-modified Mn/N co-doped biochar for tetracycline removal in environmental remediation: High-efficiency adsorption and interaction mechanisms. *J. Environ. Chem. Eng.* **2025**, *13*, 117186. https://doi.org/10.1016/j.jece.2025.117186.
128. Tavallali, A.; Mousavi, S.M.; Rabbee, M.F.; Lai, C.W.; Rahman, M.M.; Chiang, W.-H. Ionic liquids-based technologies as a sustainable agent for removing heavy metals and organic pollutants for water purification: A review. *J. Water Process Eng.* **2025**, *71*, 107367. https://doi.org/10.1016/j.jwpe.2025.107367.
129. Lin, X.; Tran, D.T.; Choi, J.-W.; Song, M.-H.; Yun, Y.-S. Ionic liquid-modified chitosan fibers for Au(I) recovery from waste printed circuit boards bioleachate: Preparation, adsorption mechanism, and application. *Sep. Purif. Technol.* **2023**, *306*, 122533. https://doi.org/10.1016/j.seppur.2022.122533.
130. Matandabuzo, M.; Ajibade, P.A. Vinyl pyridinium polymeric ionic liquid functionalized carbon nanotube composites as adsorbent for chromium(VI) in aqueous solution. *J. Mol. Liq.* **2019**, *296*, 111778. https://doi.org/10.1016/j.molliq.2019.111778.
131. Zhang, N.; Qiao, Y.; Zhang, J.; Cui, P.; Liu, X. Corn stalk biochar modified with imidazolium-based ionic liquids for the removal of $Cd^{2+}$ from mine water. *J. Environ. Sci. Health Part A* **2025**, *60*, 112–120. https://doi.org/10.1080/10934529.2025.2520168.
132. Huang, L.; Jin, Y.; Sun, L.; Chen, F.; Fan, P.; Zhong, M.; Yang, J. Graphene oxide functionalized by poly(ionic liquid)s for carbon dioxide capture. *Journal of Applied Polymer Science* **2017**, *134, 44592*. https://doi.org/10.1002/app.44592.
133. Wang, X.; Liu, Y.; Liu, X.; Zhang, C.; Song, M.; Yu, Y.; Han, X.; Li, J.; Wang, A. Facile in-situ fabrication of graphene oxide/poly(ionic liquid) composites and their adsorption performance for methyl orange. *Process Saf. Environ. Prot.* **2024**, *190*, 678–687. https://doi.org/10.1016/j.psep.2024.07.083.
134. Habila, M.A.; AlOthman, Z.A.; Ghfar, A.A.; Al-Zaben, M.I.M.; Alothman, A.A.S.; Abdeltawab, A.A.; El-Marghany, A.; Sheikh, M. Phosphonium-based Ionic Liquid Modified Activated Carbon from Mixed Recyclable Waste for Mercury(II) Uptake. *Molecules* **2019**, *24*, 570. https://doi.org/10.3390/molecules24030570.
135. Yang, G.; Huang, Q.; Gan, D.; Huang, H.; Chen, J.; Deng, F.; Liu, M.; Wen, Y.; Zhang, X.; Wei, Y. Biomimetic functionalization of carbon nanotubes with poly(ionic liquids) for highly efficient adsorption of organic dyes. *J. Mol. Liq.* **2019**, *296*, 112059. https://doi.org/10.1016/j.molliq.2019.112059.
136. Hao, Y.; Cui, Y.; Peng, J.; Zhao, N.; Li, S.; Zhai, M. Preparation of graphene oxide/cellulose composites in ionic liquid for Ce (III) removal. *Carbohydr. Polym.* **2019**, *208*, 269–275. https://doi.org/10.1016/j.carbpol.2018.12.068.
137. Nasrollahpour, A.; Moradi, S.E. Effective Removal of Hexavalent Chromium from Aqueous Solutions Using Ionic Liquid Modified Graphene Oxide Sorbent. *Chem. Biochem. Eng. Q.* **2017**, *31*, 325–334. https://doi.org/10.15255/CABEQ.2016.872.
138. Zambare, R.S.; Nemade, P.R. Ionic liquid-modified graphene oxide sponge for hexavalent chromium removal from water. *Colloids Surf. A: Physicochem. Eng. Asp.* **2021**, *609*, 125657. https://doi.org/10.1016/j.colsurfa.2020.125657.
139. Shang, J.; Guo, Y.; He, D.; Qu, W.; Tang, Y.; Zhou, L.; Zhu, R. A novel graphene oxide-dicationic ionic liquid composite for Cr(VI) adsorption from aqueous solutions. *J. Hazard. Mater.* **2021**, *416*, 125706. https://doi.org/10.1016/j.jhazmat.2021.125706.
140. Nagaraj, A.; Munusamy, M.A.; Al-Arfaj, A.A.; Rajan, M. Functional Ionic Liquid-Capped Graphene Quantum Dots for Chromium Removal from Chromium Contaminated Water. *J. Chem. Eng. Data* **2019**, *64*, 651–667. https://doi.org/10.1021/acs.jced.8b00887.
141. Ni, R.; Wang, Y.; Wei, X.; Chen, J.; Xu, P.; Xu, W.; Meng, J.; Zhou, Y. Ionic liquid modified molybdenum disulfide and reduced graphene oxide magnetic nanocomposite for the magnetic separation of dye from aqueous solution. *Anal. Chim. Acta* **2019**, *1054*, 47–58. https://doi.org/10.1016/j.aca.2018.12.037.
142. Yang, G.; Wu, Y.; Liu, M.; Liang, J.; Huang, Q.; Dou, J.; Wen, Y.; Deng, F.; Zhang, X.; Wei, Y. A novel method for the functionalization of graphene oxide with polyimidazole for highly efficient adsorptive removal of organic dyes. *J. Mol. Liq.* **2021**, *339*, 116794. https://doi.org/10.1016/j.molliq.2021.116794.
143. Xu, X.; An, X. Spherical activated carbon modified by polymerized ionic liquid for the removal of ibuprofen from water. *J. Chem. Technol. Biotechnol.* **2016**, *91*, 1794–1801. https://doi.org/10.1002/jctb.4770.
144. Gao, H.; Zhao, S.; Cheng, X.; Wang, X.; Zheng, L. Removal of anionic azo dyes from aqueous solution using magnetic polymer multi-wall carbon nanotube nanocomposite as adsorbent. *Chem. Eng. J.* **2013**, *223*, 84–90. https://doi.org/10.1016/j.cej.2013.03.004.

145. Mahurin, S.M.; Fulvio, P.F.; Hillesheim, P.C.; Nelson, K.M.; Veith, G.M.; Dai, S. Directed Synthesis of Nanoporous Carbons from Task-Specific Ionic Liquid Precursors for the Adsorption of $CO_2$. *ChemSusChem* **2014**, *7*, 3284–3289. https://doi.org/10.1002/cssc.201402338.
146. Sun, Y.; Dai, Y.; Zhu, X.; Han, R.; Wang, X.; Luo, C. A nanocomposite prepared from bifunctionalized ionic liquid, chitosan, graphene oxide and magnetic nanoparticles for aptamer-based assay of tetracycline by chemiluminescence. *Microchim. Acta* **2019**, *187*, 63. https://doi.org/10.1007/s00604-019-4012-6.
147. Sun, X.; Yang, N.; Dong, H.; Yu, H.; Yu, H.; Feng, L. In-situ electrochemical synthesis of heteroatoms-doped reduced graphene oxide toward nonradical degradation of tetracycline. *Chem. Eng. J.* **2023**, *471*, 144834. https://doi.org/10.1016/j.cej.2023.144834.
148. Xie, Z.-L.; Su, D.S. Ionic Liquid Based Approaches to Carbon Materials Synthesis. *Eur. J. Inorg. Chem.* **2015**, *2015*, 1137–1147. https://doi.org/10.1002/ejic.201402607.
149. Kuroda, K. A simple overview of toxicity of ionic liquids and designs of biocompatible ionic liquids. *New J. Chem.* **2022**, *46*, 20047–20052. https://doi.org/10.1039/D2NJ02634A.
150. Tekić, D.; Musovic, J.; Milojević-Rakić, M.; Jocić, A.; Dimitrijević, A. Innovative Green Strategy for the Regeneration of Spent Activated Carbon via Ionic Liquid-Based Systems. *Appl. Sci.* **2025**, *15*, 9880. https://doi.org/10.3390/app15189880.

processes

an Open Access Journal by MDPI

IMPACT FACTOR 2.8

CITESCORE 5.5

# CERTIFICATE OF PUBLICATION

The certificate of publication for the article titled:

A Review on Ionic Liquids in the Design of Carbon-Based Materials for Environmental Contaminant Removal

Authored by:

Tamara Terzić; Tatjana Mitrović; Marija Perović; Tamara Lazarević-Pašti

Published in:

*Processes* **2026**, Volume 14, Issue 2, 352

MDPI

Basel, January 2026

Prof. Dr. Giancarlo Cravotto
Editor-in-Chief

processes

an Open Access Journal by MDPI

# A Review on Ionic Liquids in the Design of Carbon-Based Materials for Environmental Contaminant Removal

Tamara Terzić; Tatjana Mitrović; Marija Perović; Tamara Lazarević-Pašti

*Processes* **2026**, Volume 14, Issue 2, 352